A Multi-Objective Optimization Workflow for Steam-Alternating-Solvent Heavy Oil Recovery Process Design

by

Luis Eduardo Coimbra Paniagua

A thesis submitted in partial fulfillment of the requirements for the degree of

Master of Science

in

PETROLEUM ENGINEERING

Department of Civil and Environmental Engineering
University of Alberta

Abstract

The steam alternating solvent (SAS) process involves multiple cycles of steam and solvent (e.g. propane) being injected into a horizontal well pair to produce the heavy oil. Companies are interested in these solvent-based methods, as they entail a smaller environmental footprint with reduced water usage and greenhouse gas emissions. However, the lack of understanding regarding the influences of reservoir heterogeneities, such as shale barriers, remains a significant risk for field-scale predictions. Additionally, proper design of the process in heterogeneous reservoirs is challenging because of the uncertain heterogeneity distribution and optimization of multiple conflicting objectives. In this work, a novel hybrid multi-objective optimization (MOO) workflow is developed to search a set of Pareto-optimal operational parameters for the SAS process in heterogeneous reservoirs.

The construction of the heterogeneous models involves the following steps: first, a set of synthetic homogeneous 2D is constructed using data representative of the Cold Lake reservoir; next, sequential indicator simulation is performed to construct heterogeneous models with varying shale proportions and correlation lengths. The resultant set of SAS heterogeneous models is subjected to flow simulation. A detailed sensitivity analysis is performed to examine the impacts of shale barriers on SAS production and to formulate a set of operational/decision parameters (e.g. solvent concentration, number/duration of cycles, bottom-hole pressure) and the objective functions (e.g. recovery factor and cumulative solvent injection) to be optimized. The non-dominated sorting genetic

algorithm II (NSGA-II), which is a MOO scheme, is applied to search for the optimal sets of decision parameters. To account for multiple reservoir models representing the different realizations of the shale barrier configuration, a weighted objective function, which represents an average measure over all reservoir models, is employed. Finally, to reduce the computational cost, several proxy models are included in the hybrid workflow to evaluate the defined objective functions.

The growth of a steam-solvent chamber is hampered due to the presence of shale barriers, particularly in the near-well region. These observations are consistent with those reported in several previous studies. However, the behavior of SAS may be different from the SAGD process alone, depending on the relevant solvent transport mechanisms such as dispersion. Results of the optimization workflow reveal that both the solvent concentration and duration of the solvent injection in the early cycles have significant impacts. Integrating the proposed proxy models in a hybrid optimization workflow has considerably reduced the computation requirement.

This study describes an efficient Pareto-based optimization workflow for the designing of SAS operational parameters; its main advantage is that it can consider multiple conflicting objective functions and different uncertain reservoir heterogeneity scenarios. This work offers a promising potential to de-risk solvent-based technologies for heavy oil recovery by facilitating more robust field-scale decision-making.

Preface

This thesis is composed by research previously published for two conferences: Coimbra, L., Ma, Z., & Leung, J. Y. (2019). Practical Application of Pareto-Based Multi-Objective Optimization and Proxy Modeling for Steam Alternating Solvent Process Design. In SPE Western Regional Meeting. Society of Petroleum Engineers, and Coimbra, L., Ma, Z., & Leung, J. Y. (2020). Design Of Steam Alternating Solvent Process Operational Parameters Considering Shale Heterogeneity. In Latin America and Caribbean Petroleum Engineering Conference (LACPEC). Society of Petroleum Engineers. I was responsible for the coding development, result analysis, and manuscript preparation.

Chapter 1 is originally written by Luis Coimbra and has not been published before. Chapters 3-5 are derived from papers submitted to peer-reviewed journals.

I dedicate this work to God, and to my beloved mother and sister, who always supported and motivated me on my way throughout this journey.

Acknowledgments

First and foremost, I would like to extend my sincere gratitude to my supervisor, Dr. Juliana Leung, for the huge opportunity she gave me to achieve my professional goals working in her group research. She was the light all the way until the end, she helped me find my way when I even doubt about myself, and her guidance, unlimited patience, and insightful ideas during the entire research was pivotal to complete this thesis.

I also would like to thank my defense committee, Dr. Zhehui Jin, Dr. Yashar Pourrahimian, and Dr. Douglas Tomlinson, for their insightful suggestions and comments.

Finally, I would like to express my gratitude to my country. I would never have imagined being in this program without the support of the education authorities.

Table of Contents

Abstract ii

Preface iv

Acknowledgments vi

Table of Contents vii

List of Tables x

List of Figures xii

List of Symbols xv

Chapter 1 Introduction 1

1.1 Background 1

1.2 Problem Statement 3

1.3 Research Objectives 3

1.4 Thesis Outline 4

Chapter 2 Literature Review 6

2.1 Steam-solvent hybrid processes 6

2.2 Fundamentals of the Steam Alternating Solvent Process 6

2.2 Multi-objective Optimization Approaches 9

Chapter 3 Research Methodology 12

3.1 SAS Model Description 12

3.2 Heterogeneity Modeling 20

3.3 Proposed Hybrid MOO Workflow 23

Chapter 4 Practical Application of Pareto-Based Multi-Objective Optimization and Proxy Modeling for Steam Alternating Solvent Process Design 24

4.1 Selection of Decision Parameters and Objective Functions 24

4.2 Fundamentals of MOO 26

4.3 Non-dominated sorting genetic algorithm-II (NSGA-II) 28

4.4 Construction of Proxy Models: Response Surface Method 29

4.5 Results and Discussion 30

4.5.1 Response Surface (Proxy) Modeling 30

4.5.2 Optimization Results and Discussions 33

4.5.2.1 Two-objectives optimization 33

4.5.2.2 Three-objectives optimization 37

Chapter 5 Design of Steam Alternating Solvent Process Operational Parameters Considering Shale Heterogeneity 46

5.1 Selection of Decision Parameters and Objective Functions 46

5.2 Introduction of MOO and Non-Dominated Sorting Genetic Algorithm-II (NSGA-II) 47

5.3 Construction of Response Surface Proxy Models 50

5.4 Proposed Hybrid MOO Workflow 51

5.5 Results and Discussion 53

5.5.1 Response Surface (Proxy) Modeling 53

5.5.2 Optimization Results and Discussions 54

Chapter 6 Conclusions and Recommendations 64

6.1 Conclusions 64

6.2 Recommendations 65

References 66

Appendices 72

List of Tables

Table 3.1—Parameters used in field-scale numerical simulations. 13

Table 4.1—Summary of the objective functions corresponding to the initial set of 144 SAS cases used for proxy modeling. 26

Table 4.2—NSGA-II settings. 29

Table 4.3—Experimental design: ranges and step sizes of the decision variables for proxy modeling. 30

Table 4.4—Initial ranges of decision parameters and objective functions prior to optimization. 34

Table 4.5—Final ranges of decision parameters and objective functions after optimization. 35

Table 4.6—Proposed ranges of decision parameters and objective functions after optimization. 36

Table 4.7—Final ranges of decision parameters after optimization (3 objective functions). 43

Table 5.1—Summary of the objective functions corresponding to the initial set of 144 SAS cases of one randomly-selected heterogeneous reservoir used for proxy modeling. 47

Table 5.2—NSGA-II configuration. 50

Table 5.3—Experimental design: ranges and step sizes of the decision variables for proxy (RSM) modeling. 51

Table 5.4—Experimental design: ranges and step sizes of the decision variables for proxy (RSM) modeling. 54

Table 5.5—Final ranges of objective functions after optimization and decision parameters. 55

List of Figures

Figure 2.1—Schematic of the base SAS simulation model. 8

Figure 2.2—Schematic of the NSGA-II procedure (Deb 2001). 10

Figure 3.1—Schematic of the proposed SAS model. 13

Figure 3.2—Production profiles (q = monthly average oil production rate; RF = recovery factor) from the base SAS model. 15

Figure 3.3—Oil saturation (S_o, fraction) at different injection times: green color denotes the steam-solvent chamber. The SAS phase starts after 2 years. 16

Figure 3.4—Oil saturation, S_o [fraction], reservoir temperature, T [°C] and gas mole fractions of methane, propane and water at: (1) end of solvent injection in cycle 1 (839 days), (2) end of steam injection in cycle 4 (1439 days), (3) end of solvent injection in cycle 9 (2279 days), and (4) end of steam injection in cycle 12 (2879 days). 17

Figure 3.5—Production rate and BHP profiles during part of the first SAS cycle (the injected fluid is switched from solvent to steam at 839 days). 19

Figure 3.6— Production rate and temperature profiles during part of the first SAS cycle (injected fluid is switched from solvent to steam at 839 days). 19

Figure 3.7—Oil saturation corresponding to four randomly-selected heterogeneous cases (blue – shales; red – sand) at different times: a) end of SAGD (719 days), b) end of SAS cycle 6 (1799 days), and c) end of SAS cycle 12 (2879 days). 21

Figure 3.8—RF of the homogeneous case and the four randomly-selected heterogeneous cases (blue – shales; red – sand). 22

Figure 3.9—Oil Saturation at 2880 days for the homogeneous case and heterogeneous case #2..... 22

Figure 3.10—Flow diagram of the Hybrid SAS optimization process..... 23

Figure 4.1—Comparison between the flow simulation data and the predicted values from RSM proxy model: top row: two objective functions; bottom row: three objective functions..... 32

Figure 4.2—Pareto-optimal front for the SAS process: a) first iteration; b) last iteration: blue – region (a); red – region (b). 33

Figure 4.3—Histograms of decision parameters: blue – region (a); red – region (b)..... 34

Figure 4.4— Selected cases (red) along the Pareto-optimal front for the SAS process. .. 36

Figure 4.5— Histograms of decision parameters of the 93 "most optimal" results: blue – region (a); red – region (b). 37

Figure 4.6—Pareto-optimal front for the SAS process: black circles – initial population, colored circles – final population: blue – region (a); red – region (b); green – region (c). 39

Figure 4.7—Projections of the Pareto-optimal front for the SAS process onto three 2D planes for the final population: i) 1/RF vs $Q_{propane}$; ii) 1/RF vs Q_{water} iii) Q_{water} vs $Q_{propane}$ [blue – region (a); red – region (b); green – region (c)]..... 40

Figure 4.8— Histograms of decision parameters: blue – region (a); red – region (b); green – region (c). 43

Figure 5.1—Flow diagram of the Hybrid SAS optimization process with the consideration of reservoir heterogeneity. 52

Figure 5.2—Comparison between the flow simulation data and the predicted values from RSM proxy model for one of the heterogeneous cases (case 5). 53

Figure 5.3—Pareto-optimal front for the SAS process for the last iteration corresponding to the three different overall objective function formulations. 55

Figure 5.4—Pareto-front and histograms of decision parameters when the overall objective function is computed as the average among all 10 heterogeneous realizations: blue – region (a); red – region (b). 58

Figure 5.5—Pareto-front and histograms of decision parameters when the overall objective function is computed as the minimum among all 10 heterogeneous realizations: blue – region (a); red – region (b). 59

Figure 5.6—Pareto-front and histograms of decision parameters when the overall objective function is computed as the maximum among all 10 heterogeneous realizations: blue – region (a); red – region (b); green – new cluster. 61

List of Symbols

β_i = *regression coefficient*

$\boldsymbol{\beta}$ = *a vector of regression coefficients*

cSOR: cumulative steam-oil ratio, m^3/m^3

$\mathbf{f}(\mathbf{x})$ = *objective functions vector*

$\mathbf{x}$ = *decision variable vector*

GOR = gas-oil ratio, m^3/m^3

GOR = gas/oil ratio, fraction

q = *oil production rate,* m^3

RF = recovery factor, fraction

S_o = *oil saturation, fraction*

T = *temperature,* ^oC

BHP = bottom-hole pressure, kPa

$F_{propane}$ = *Fraction of propane, solvent composition*

T_{early} = *duration of solvent injection in each cycle of the early SAS stage, months*

T_{late} = *duration of solvent injection in each cycle of the late SAS stage, months*

$Propane_{retention}$ = *propane (solvent) retention, fraction*

$Q_{propane}$ = *cumulative propane injected normalized, fraction*

Q_{water} = *cumulative steam injected normalized, fraction*

$V_{propane}^{inj}$ = *volume of injected propane,* m^3

$V_{propane}^{prod}$ = *volume of produced propane,* m^3

$V_{propane\_max}^{inj}$ = *maximum volume of injected propane,* m^3

$g_j(\mathbf{x})$, $h_k(\mathbf{x})$ = *constraint functions*

ψ^j = *average crowding distance, fraction*

N_k = *number of solutions in the* k^{th} *non-dominated front*

R^2 = *coefficient of determination*

Acronyms

MOO = Multi-objective optimization

NSGA-II = Non-dominated Sorting Genetic Algorithm II

POF = Pareto-optimal front

RSM = Response Surface Model

SAGD = Steam Assisted Gravity Drainage thermal recovery process

SAP = Solvent Aided Process

SA-SAGD = Solvent Assisted Steam Assisted Gravity Drainage

SAS = Steam Alternating Solvent process

VAPEX = Vapor Extraction

SISIM = Sequential Indicator Simulation

GSLIB = Geostatistical Software Library

Chapter 1 Introduction

1.1 Background

The oil sand deposits in the province of Alberta, Canada, are considered among the world's largest crude oil resources, with an estimated volume of 1.845 billion barrels of oil equivalent (Alberta Energy Regulator, 2014). Approximately 20% of the resources can be produced via strip mining, while the remaining 80% must be developed via in-situ enhanced oil recovery (EOR) techniques, such that either thermal energy or solvents must be injected (Souraki et al., 2013).

Examples of thermal-based methods include hot water flooding, cyclic steam stimulation (CSS) (Ali and Blunschi, 1983), steam-assisted gravity drainage (SAGD) (Butler et al., 1981), in-situ combustion (Martin et al., 1958), and steam injection (Donaldson et al., 1989). For these types of processes, thermal energy is added to reduce the oil viscosity, such that the diluted oil can flow into the producer. SAGD has evolved to become one of the most popular techniques for commercial bitumen extraction, where high-temperature and high-pressure steam is continuously injected into a horizontal injector, the diluted bitumen, as well as the condensed water, would drain along the chamber edge via gravity towards another horizontal well that is located at a few meters below the injector. Common disadvantages associated with most steam-based thermal methods are the high energy and water consumption (i.e. the energy requirement for heating the water to get saturated steam), significant greenhouse gas (GHG) emissions (by-products in the combustion of natural gas to generate steam, measured the GHG intensity

in kg CO_{2eq}/bbl of bitumen produced), and potential heat loss to the over- and under-burden. Therefore, alternative solvent-based techniques have been proposed, where low molecular-weight hydrocarbons (e.g., propane, butane) mixtures are added for viscosity reduction. The physical mechanisms involved are molecular diffusion and dispersion, instead of latent heat transfer in thermal methods. The vapor-extraction process (VAPEX) utilizes the same well configuration as in SAGD, but a solvent mixture, instead of steam, is injected (Butler and Mokrys, 1991). However, its field-scale implementation remains challenging because of the slow rate of mass transfer (Leung, 2014; Shi et al., 2014).

Generally speaking, solvent-assisted processes could offer important potential for reducing the environmental footprint, but the corresponding oil production rates are generally much lower and the challenges of solvent recovery or recycling are serious obstacles. To capitalize on the synergy of SAGD and VAPEX techniques, many hybrid heavy oil recovery techniques have been proposed.

The process of steam alternating solvent, or SAS, utilizes the same well configuration as in the conventional SAGD scheme; however, cycles of steam and solvent are injected in an alternating fashion (Zhao, 2007). The SAS process is deemed to be more energy-efficient and environment-friendly with less greenhouse gas emission and water usage. However, proper design of the SAS process is challenging as multiple conflicting objectives need to be optimized simultaneously. Conventional optimization methods that aggregate multiples objectives into a single weighted objective are not appropriate.

In this work, a novel workflow is developed to identify a set of Pareto-optimal operational parameters for the SAS process, in homogeneous and heterogeneous reservoirs.

1.2 Problem Statement

The SAS process was originally proposed as an alternative that combines the advantages of the steam-assisted gravity drainage (SAGD) and vapor extraction (VAPEX) (Zhao 2007). The process asses its performance for a particular homogeneous reservoir with fixed operational parameters. The author suggested to find or determine de desired profiles by looking at the operational parameters of the process.

It is also important to remark that realistic cases present reservoir heterogeneities, which are not considered in the proposed paper. It is important to consider heterogeneous reservoirs in order to adequately propose the operational parameters to carry out the project.

The complexity of the process leads to require high computational efforts to optimize the process due to the conflicting objectives that this process inherit, an optimization framework has not yet been presented. It is for that reason that this study proposes a novel hybrid optimization workflow that can answer this statement: “Can the SAS process be designed with optimum parameters in order to improve its efficiency?”

1.3 Research Objectives

The general objective of this study is to propose a hybrid multi-objective optimization of a set of Pareto-optimum solutions with considerable savings in computational costs for

homogeneous and heterogeneous reservoirs. For this goal, the specific objectives are presented:

(1) To build a base SAS model and perform a systematic sensitivity analysis
(2) To construct proxy models that contributes in the computing efficiency of the optimization of the process
(3) To implement a multi-objective optimizer to calculate the objective functions
(4) To analyze and demonstrate the feasibility of the proposed operational parameters obtained in the Pareto fronts

1.4 Thesis Outline

This thesis consists of six chapters. The outline of these chapters is provided as follows:

Chapter 1 presents the introduction to the study composed by background, the aspects related to the SAS process, the problem statement, and the objectives of the thesis.

Chapter 2 presents the literature review related to the solvent assisted thermal recovery processes for heavy oil, the response surface methodology, and the multi-objective optimization approaches.

Chapter 3 presents the methodology implemented to develop the workflow of multi-objective optimization of the SAS process.

Chapter 4 presents the application of the workflow to a homogeneous reservoir.

Chapter 5 presents the updated workflow to perform multi-objective optimization in heterogeneous reservoirs.

Chapter 6 presents the conclusions and recommendations.

Chapter 2 Literature Review

2.1 Steam-solvent hybrid processes

In recent years, corporate and academia research have advocated the development of processes derived from the SAGD process implementing the addition of solvents. Solvent Aided Process (SAP) (Gupta and Gittins, 2006) utilizes butane as a solvent, predicting a reduction of steam requirement of 30% compared to the conventional SAGD (Cenovus Energy, n.d.). Imperial Oil conducted a research of the Solvent Assisted SAGD (SA-SAGD) claiming 25% of GHG intensity reduction with a corresponding reduction of steam requirement of 25% (Imperial Oil, n.d.). These hybrid methods co-inject solvent with the steam, but a variation of them have been proposed: The Steam Alternating Solvent (SAS) Process.

2.2 Fundamentals of the Steam Alternating Solvent Process

The SAS process was first proposed by Zhao (2007), where steam and solvent are alternatively injected using the same well configuration as in SAGD. According to Zhao (2007), the SAS process consists of three main steps:

- Preheating the reservoir to establish a vertical communication between two wells;
- Injecting steam (as in the SAGD process) until a steam chamber is fully developed and heat loss to overburden becomes significant;
- Implementing an injection cycle in which solvent and steam are injected alternatively: solvent injection for a few months is followed by steam injection for

another few months. The entire production life is divided into numerous cycles. It should be noted that the production continues during the entire operation, and no soaking/shut-in periods are necessary.

Zhao explained that the injected solvent should have a dew point temperature between the initial reservoir temperature and the steam temperature at the operating pressure. The particular advantage of the alternate injection pattern compared to co-injecting solvent and steam, according to Zhao, is that SAS could help to reduce solvent retention by disturbing the potential solvent accumulation around or below the producer well.

The set-up of the computational domain of the SAS process is illustrated in Figure 2.1. A proper design of the SAS process is challenging, as multiple conflicting objectives, such as maximizing recovery factor and minimizing cumulative solvent injection, should be considered simultaneously. Accounting for these objectives is necessary to formulate a set of optimal operational parameters to maximize project economics and to reduce environmental impact in a field operation. Numerous parameters can affect the overall solvent efficiency: types of solvent, solvent concentration, duration of solvent injection in each cycle. Other relevant operational constraints may include flowing bottom-hole pressure or bottom-hole gas production. In this study, a sensitivity analysis was carried out, and it was identified that the fraction of propane in the injected solvent mixture and the duration of solvent injection in each cycle are the most influencing factors. Hence, these parameters are selected as decision variables for the optimization workflow.

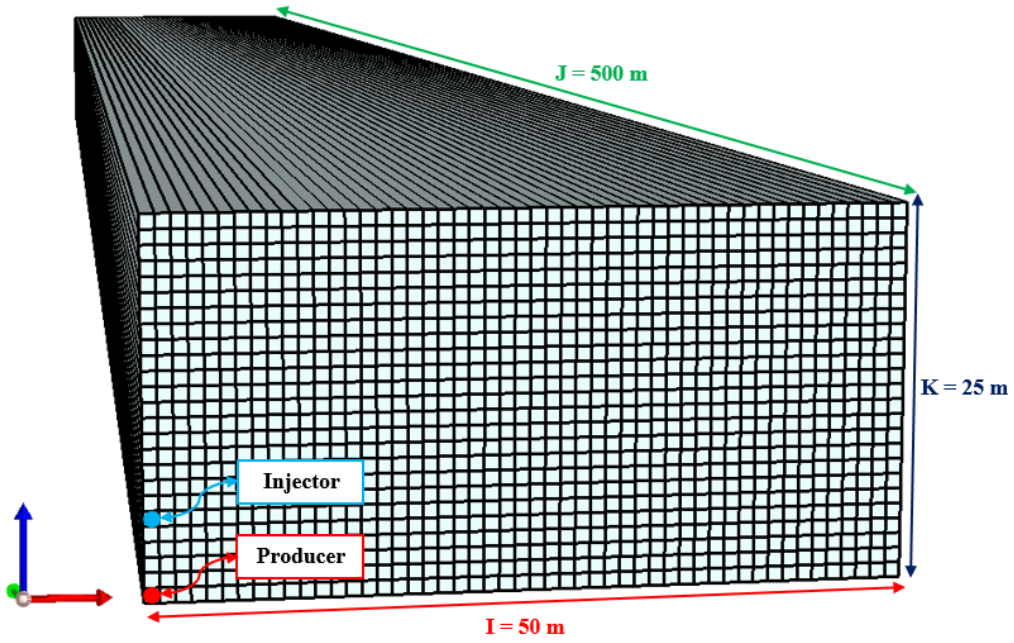

Figure 2.1—Schematic of the base SAS simulation model.

The major objective of this work is to gain additional insights regarding the optimal SAS operating conditions in homogeneous reservoirs and in the presence of shale heterogeneity. Previous studies have demonstrated that reservoir heterogeneities could adversely impact the SAGD performance (Amirian et al., 2014; Wang and Leung, 2015; Ma et al., 2018; Zheng et al., 2018; 2019), but the impacts of heterogeneities on the design of SAS operating parameters is not well understood. A hybrid workflow integrating the NSGA-II MOO scheme and response surface modeling is employed, and its application to optimize the SAS process considering heterogeneity uncertainties is novel. To the best of the authors' knowledge, the effects of uncertain shale barrier configurations on the design of SAS process has not been published.

2.2 Multi-objective Optimization Approaches

Conventional single-objective optimization methods that aggregate multiples objectives into a single weighted objective are not appropriate because, when it is used a global objective function, the solution tends to minimize the single objective regardless of the characteristics of individual objective functions. In addition, there is no universal formulation for determining the appropriate weights for each objective function (Min et al., 2017). Al-Gosayir et al. (2012) applied several hybrid techniques involving genetic algorithm (GA) to optimize the solvent-assisted SAGD processes in a heterogeneous reservoir. Their method was later adopted to study the steam-over-solvent (SOS-FR) injection in fractured reservoirs process (Al-Gosayir et al., 2013), and the results illustrated that optimizing both injection time and number of cycles using a single-objective genetic algorithm was quite challenging.

Many recent studies have advocated for the use of multi-objective optimization (MOO) approaches to provide a set of diversified solutions in terms of optimal decision parameters, when multiple conflicting objective functions are involved. MOO aims to assess the trade-off among solutions corresponding to numerous conflicting objectives, and the set of solutions (i.e., representing different combinations of optimal decision parameters) is referred to as the multi-dimensional optimal solution domain or the Pareto-optimal front (POF). In other words, the goal of a MOO scheme is to identify a set of acceptable trade-off solutions along the POF. Examples of widely-adopted MOO techniques may include vector evaluated genetic algorithm (VEGA), multiple objective

genetic algorithm (MOGA), non-dominated sorting genetic algorithm (NSGA), non-dominated sorting genetic algorithm II (NSGA-II), Niched-Pareto genetic algorithm.

MOO has also been applied to design EOR processes for heavy oil recovery in recent years. Min et al. (2017) employed a hybrid optimization approach, which integrated MOO and response surface modeling, to optimize the expanding solvent-steam assisted gravity drainage process. Ma and Leung (2019) optimize various injection parameters for the warm solvent injection process. Due to its widely-reported robust performance in a variety of applications, NSGA-II is employed as the main MOO technique in this research. Figure 2.2 shows the schematic of the NSGA-II procedure, in which the non-dominated sorting and the crowding distance sorting are the main features. This will be discussed in the following chapter.

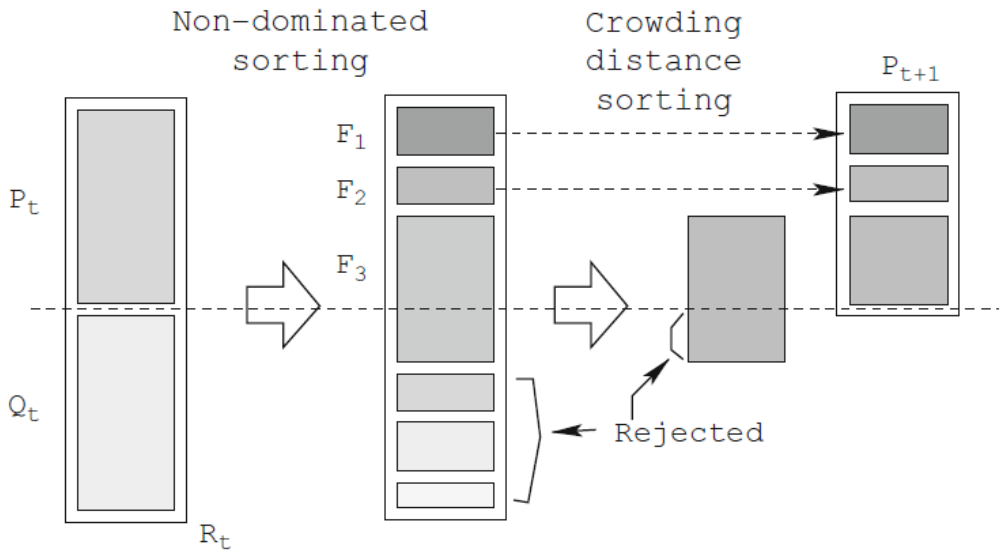

Figure 2.2—Schematic of the NSGA-II procedure (Deb 2001).

In order to reduce the computational costs associated with the objective function evaluation, proxy models approximating the non-linear relationships between the decision parameters and objective functions are constructed following the response surface method. The formulas and details regarding this technique will be discussed in the following chapters.

Chapter 3 Research Methodology

3.1 SAS Model Description

A homogeneous 2D base SAS model is constructed in accordance to realistic field data gathered from the Cold Lake reservoir, Alberta, Canada, as presented in Zhao, 2007. The well configuration in *x*-*z* plane is shown in Figure 3.1, in which two horizontal wells are placed at the bottom of the pay zone; the horizontal well trajectory is aligned with the y-axis (i.e., Δy = 500 m). Assuming symmetrical growth and development of the steam/solvent chamber, only half of a typical well pair distance of 100 m is simulated. Table 3.1 summarizes the relevant simulation parameters.

The rock-fluid properties were taken from Ma et al. (2018), such as the molar diffusion coefficient of propane in liquid of 4.32×10^{-4} m^2/day and the mechanical dispersion coefficient of 2.33×10^{-3} m The information of the oil and propane properties and propane solubility taken from Ma was not available in Zhao due to the fact that it was generated a phase property program, and no more details were given regarding to that data.

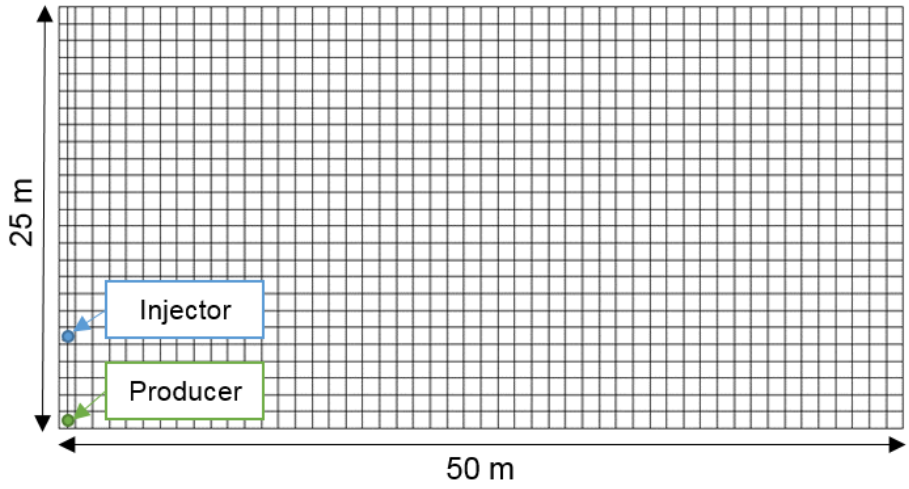

Figure 3.1—Schematic of the proposed SAS model.

Table 3.1—Parameters used in field-scale numerical simulations.

Parameter	Value
Number of grid blocks (I × J × K)	50 × 1 × 25
Size of grid block ($\Delta x \times \Delta y \times \Delta z$) (m)	1 × 500 × 1
Distance between heel and toe of horizontal wells (m)	500
Initial pressure (kPa)	3100
Initial temperature (°C)	12
Porosity (fraction)	0.33
Pay-zone thickness (m)	25
Permeability, horizontal (D)	2.5
Permeability, vertical (D)	1.5
Initial oil saturation	0.85
Oil viscosity at 12°C (cP)	47956
Oil viscosity at 220°C (cP)	4.6
Initial GOR	3.4

As discussed in the introduction, the entire SAS process (spanning over a total of 2880 days) can be divided into three phases. After the initial pre-heating phase of 90 days, steam with 95% quality is injected into the formation for two years during the SAGD phase at a constant injection pressure of 3400 kPa and temperature of 237 °C. To prevent the production of live steam, a steam trap of 2 °C is imposed. Once the steam chamber is fully established and reaches the overburden (top of the pay zone), the third phase of cyclic steam alternating solvent operation begins. The duration of each cycle is fixed as 6 months. For the base case, each cycle consists of a 4-month injection of solvent and a 2-month injection of steam. A total of 12 cycles is modeled. In order to facilitate the optimization workflow by limiting the number of decision variables, these 12 cycles are divided into 2 stages: early SAS and late SAS. Following the recommendation of Zhao (2007), a solvent mixture of 20 mol% methane and 80 mol% propane is selected for the base case. In each cycle, both solvent and steam are injected at 3400 kPa, while a maximum bottom-hole gas rate of 5 m^3/day is imposed at the producer during the solvent injection and a 2 °C steam trap is imposed during the steam injection.

The base case is subjected to flow simulation using a thermal simulator (CMG STARS, 2019). The oil production rate (q), recovery factor (RF), and the duration of each cycle for the base model is shown in Figure 3.2. The highest oil production rate occurs during the SAGD phase, whereas the original paper by Zhao (2007) reported that the peak oil production was at the beginning of the first SAS cycle. This discrepancy was also observed in a laboratory setting (Zhao et al., 2005), and it was not fully understood. However, all the results seem to suggest that the highest oil production would take place near the end of the

SAGD phase or at the beginning of the SAS phase, during which the reservoir temperature near the well pair is high and the injected fluids do not have to travel far to reach the chamber edge (i.e., solvent/steam/oil interface). Nevertheless, comparing to the production profiles presented in Zhao (2007), it is clear that many salient production characteristics, such as the fluctuations in oil production, are sufficiently captured in the base model. In addition, the predicted chamber development is presented in Figure 3.3.

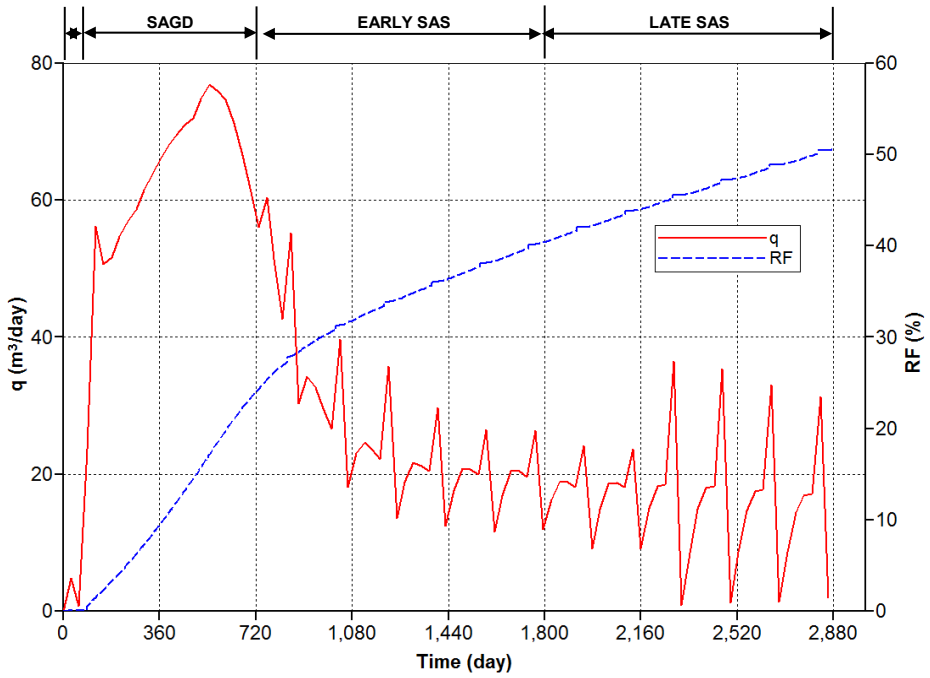

Figure 3.2—Production profiles (q = monthly average oil production rate; RF = recovery factor) from the base SAS model.

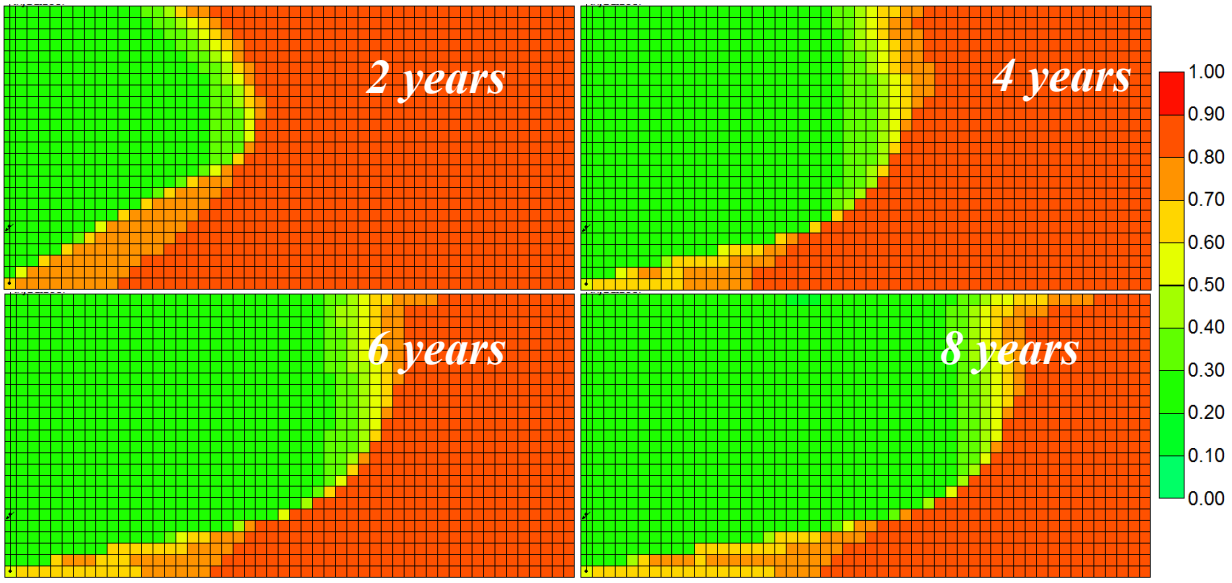

Figure 3.3—Oil saturation (S_o, fraction) at different injection times: green color denotes the steam-solvent chamber. The SAS phase starts after 2 years.

When assessing the SAS process performance, temperature distribution alone is no longer an indication of the depleted zone, as it would have been for SAGD. The reason is that only a portion of the depleted zone is expected to be at the steam temperature, reflecting an uneven distribution of temperature in the developed vapor chamber; temperature gradients may enhance solvent transport within the chamber (Zhao 2007). Figure 3.4 shows that the highest concentration of propane is along the chamber boundary, where it dissolves into the oleic phase. It can also be observed that the methane tends to accumulate near the top of the reservoir. It is clear that the zones with the highest temperature correspond to the areas with higher steam concentration (i.e., water mole fraction in the gaseous phase). The solvent mixture travels ahead of the steam to the chamber edge, where it mixes with the oil; as a result, the total chamber size is larger than the volume being at the steam temperature.

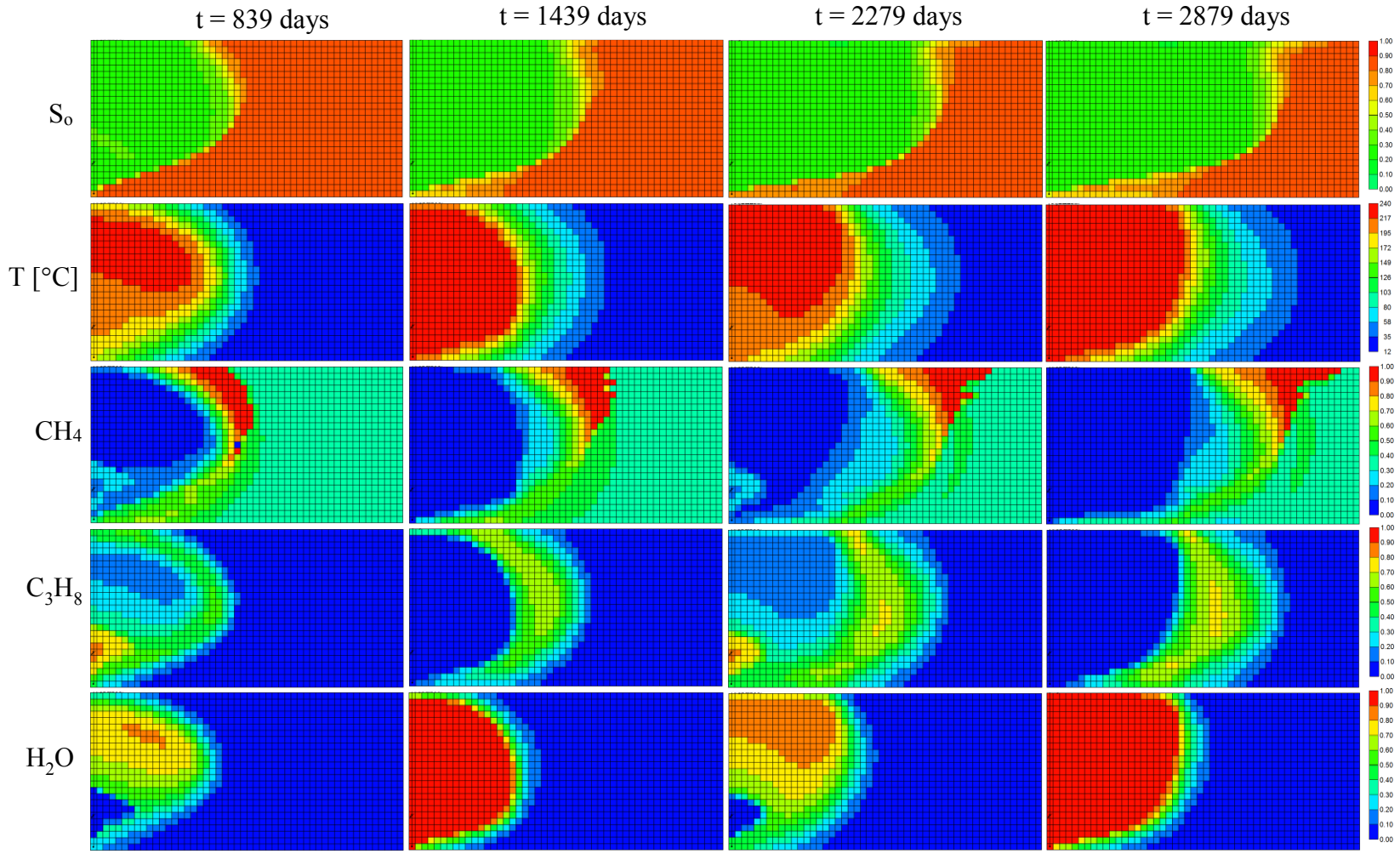

Figure 3.4—Oil saturation, S_o [fraction], reservoir temperature, T [°C] and gas mole fractions of methane, propane and water at: (1) end of solvent injection in cycle 1 (839 days), (2) end of steam injection in cycle 4 (1439 days), (3) end of solvent injection in cycle 9 (2279 days), and (4) end of steam injection in cycle 12 (2879 days).

The production, BHP and temperature profiles during part of the first SAS cycle is examined in Figures. 3.5-3.6. At the transition from solvent injection to steam injection at 840 days, there is a spike in each of the producing fluid profiles and the producer temperature. This spike coincides with a sudden drop in BHP during the first few hours immediately after the switch, and it rises again to approximately 3400 kPa. The sudden drop in BHP may be attributed to certain numerical instability associated with the abrupt change in well constraint: during the solvent injection period, the producer is operated with a constraint of maximum bottom-hole gas rate of 5 m^3/day (Figure 3.5), and the chamber temperature has been reduced (Figure 3.4); when the steam is injected again, it takes some time for the near-well temperature to rise, the steam-trap constraint to be re-established, and the producer BHP to rise back to the 3400 kPa level; in fact, immediately after the spike, there is essentially no fluid production for almost three days.

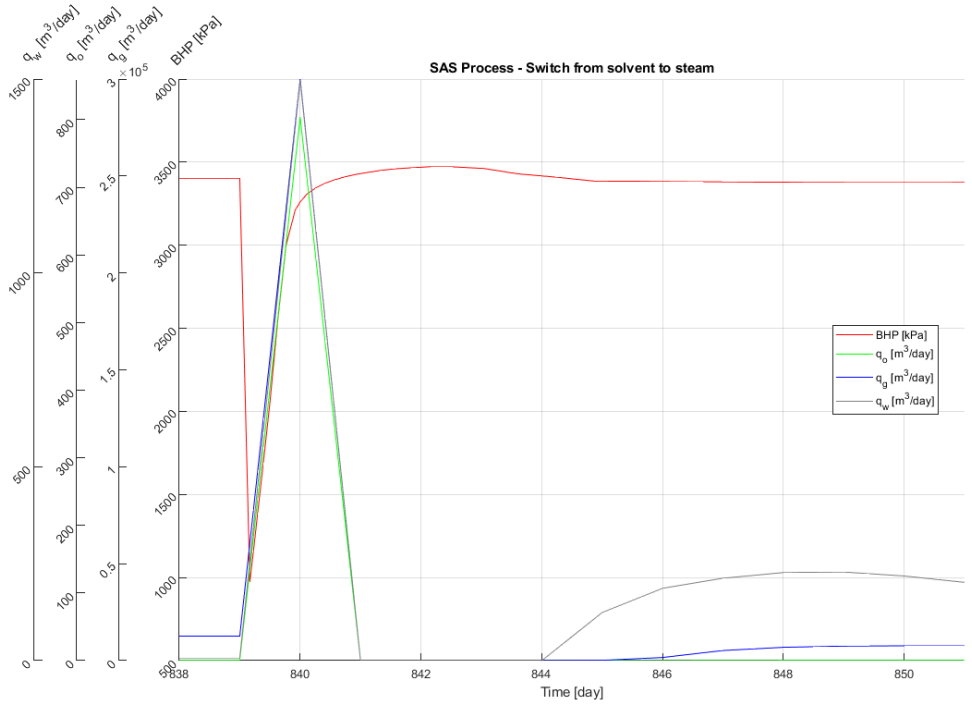

Figure 3.5—Production rate and BHP profiles during part of the first SAS cycle (the injected fluid is switched from solvent to steam at 839 days).

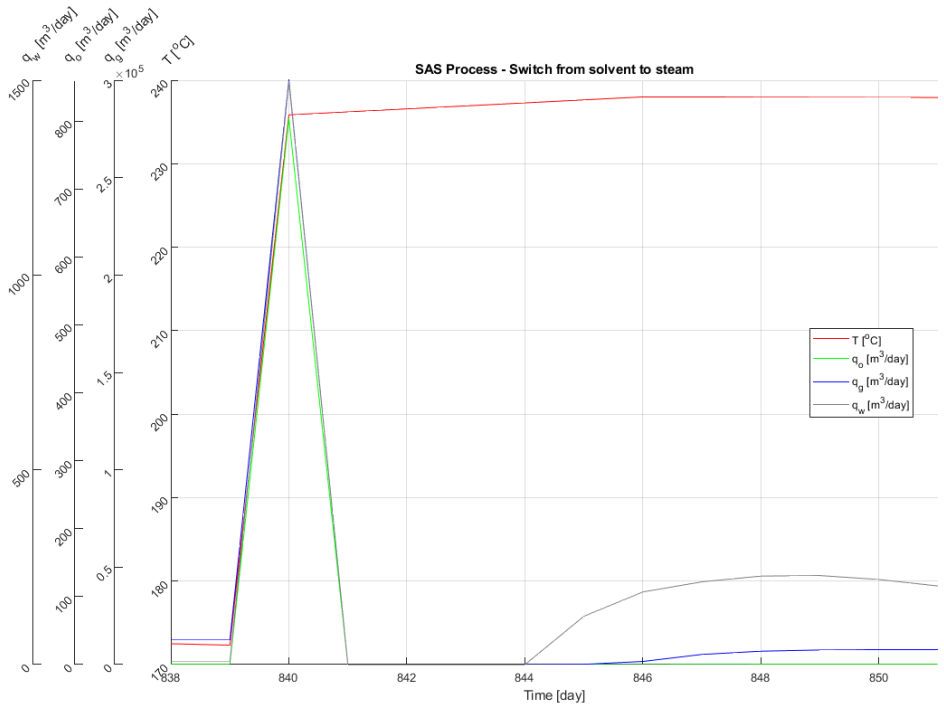

Figure 3.6— Production rate and temperature profiles during part of the first SAS cycle (injected fluid is switched from solvent to steam at 839 days).

3.2 Heterogeneity Modeling

The effects of shale barriers on the SAS process are examined. Realizations of shale barrier distribution are generated stochastically based on the Sequential Indicator Simulation (SISIM) technique, as implemented in the Geostatistical Software Library (GSLIB) by Deutsch and Journel (1992). Each realization consists of 10% of shale by volume; ranges for the semivariogram are 20 m along the direction of maximum anisotropy (azimuth angle of 75°) and 2 m along the direction of minimum anisotropy. The grid cells where the injector and producer are located consist of sand only.

Figure 3.7 presents four randomly selected heterogeneous models and their corresponding oil saturation profiles at various times. It is clear that the shale barriers could hamper the chamber development, but the specific impacts of these heterogeneous features would depend on spatial arrangement of the shale barriers in each model; for example, a cluster of shale barriers located right above the injector (e.g., case #2) would have a more dramatic effect on the steam chamber growth than the other models.

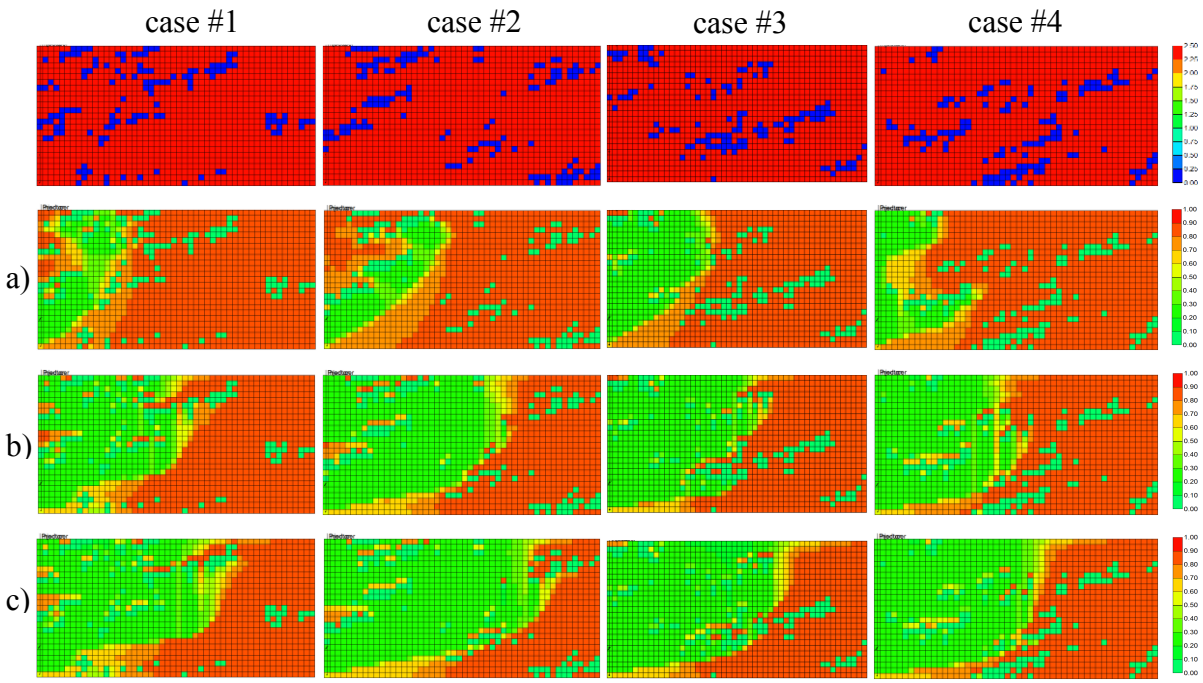

Figure 3.7—Oil saturation corresponding to four randomly-selected heterogeneous cases (blue – shales; red – sand) at different times: a) end of SAGD (719 days), b) end of SAS cycle 6 (1799 days), and c) end of SAS cycle 12 (2879 days).

The recovery performance for four of the heterogeneous cases are compared with the homogeneous model in Figure 3.8. Cases #1, 2 and 4 yield relatively lower recoveries during the SAGD period, as the presence of shale barriers in the near-injector region would severely impact the chamber development, particularly along the vertical direction. However, during the solvent injection cycles, a RF of 50.76%, which is nearly identical to that corresponding to the homogeneous case (50.85%), is attained for case #2. It appears that the heterogeneities may introduce additional mixing near and ahead of the chamber edge, enabling the drained area to grow faster in the heterogeneous case, as shown in Figure 3.9. This observation is corroborated by previous simulation studies involving other solvent-injection process (e.g., VAPEX) (Leung, 2014).

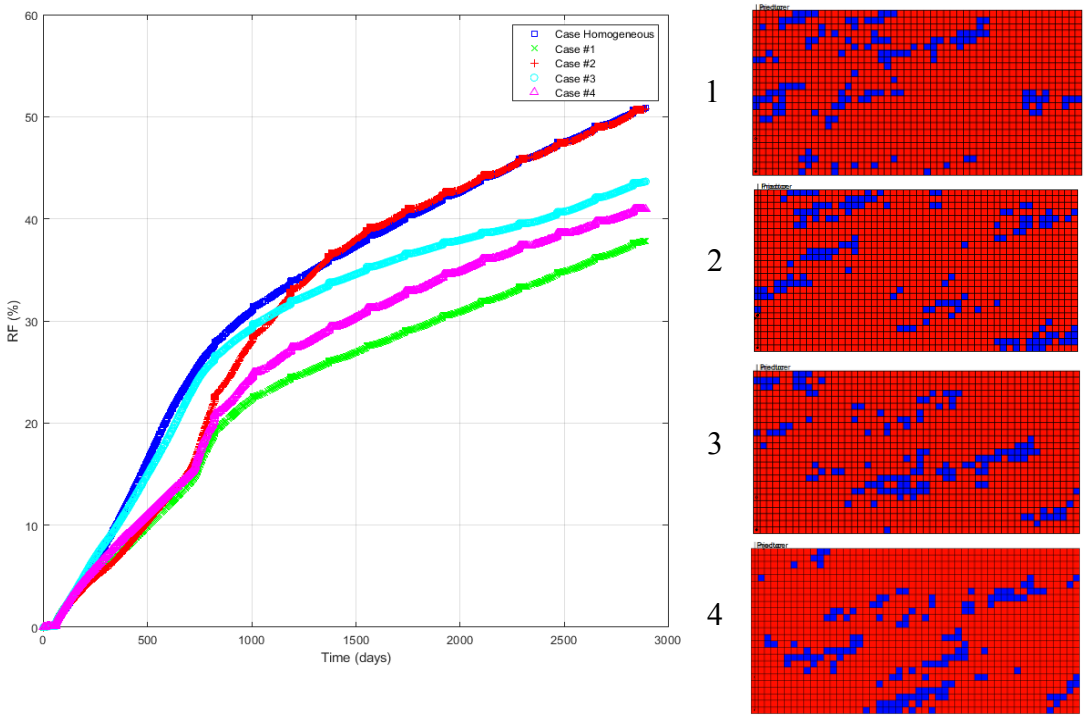

Figure 3.8—RF of the homogeneous case and the four randomly-selected heterogeneous cases (blue – shales; red – sand).

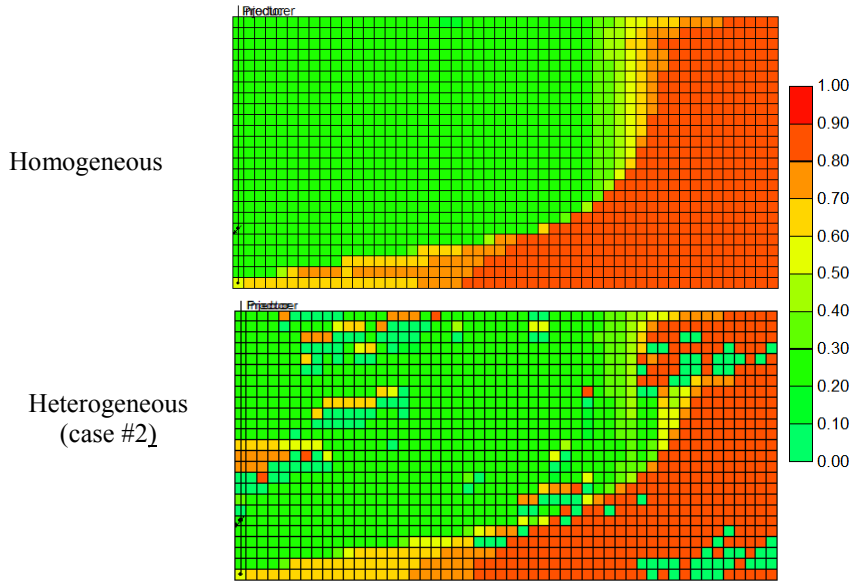

Figure 3.9—Oil Saturation at 2880 days for the homogeneous case and heterogeneous case #2.

3.3 Proposed Hybrid MOO Workflow

The proposed workflow applied in this work is illustrated in Figure 3.10. Several remarks should be made: (1) sensitivity analysis should be conducted to identify the appropriate decision parameters and the corresponding objective functions. (2) The accuracy and robustness of the trained proxy models should be assessed. At the end, a set of Pareto-optimal decision parameters and the corresponding objective function values are computed.

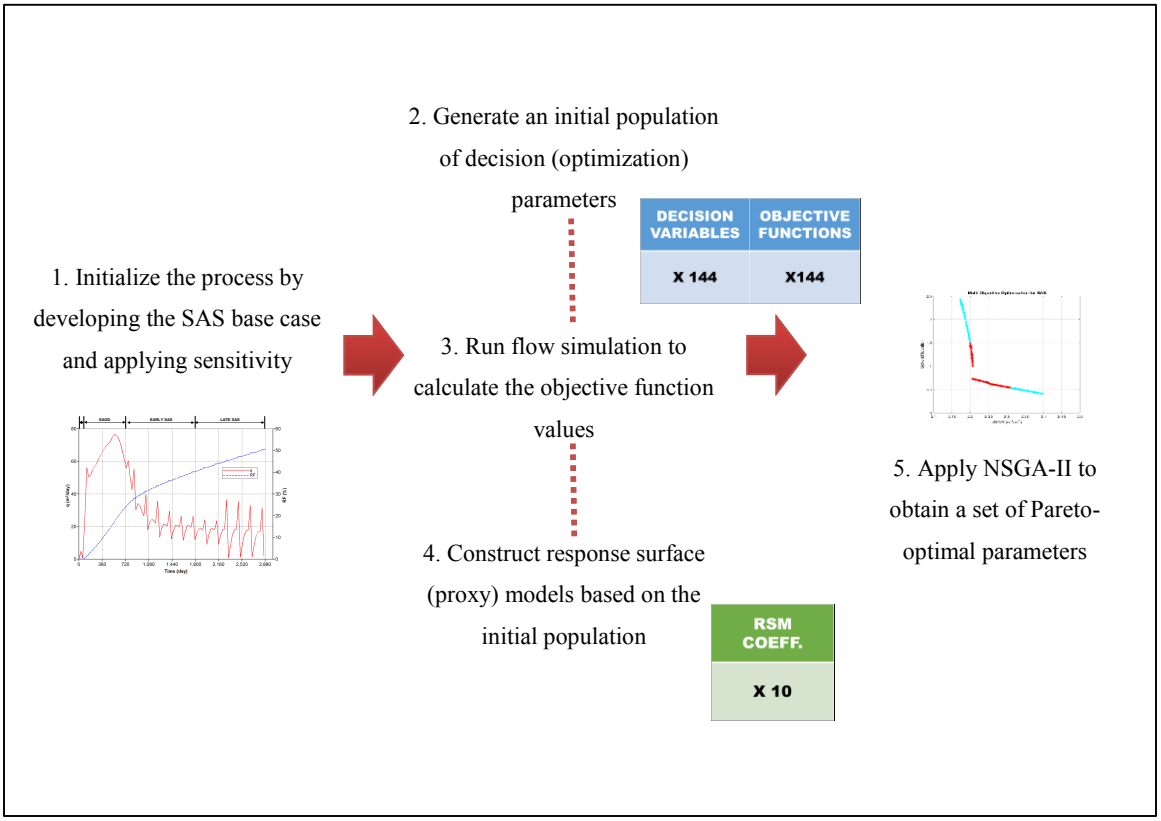

Figure 3.10—Flow diagram of the Hybrid SAS optimization process.

Chapter 4 Practical Application of Pareto-Based Multi-Objective Optimization and Proxy Modeling for Steam Alternating Solvent Process Design

4.1 Selection of Decision Parameters and Objective Functions

A detailed sensitivity analysis is conducted to determine the appropriate decision variables and objective functions. Appendix 1 presents the sensitivity analysis for several decision parameters, including the composition of injected solvent, the temperature of injected fluids, the bottom-hole pressures of injector and producer, the steam trap temperature, the bottom-hole gas produced, and different patterns of solvent injection in the cycling period. The results reveal that the SAS process performance is most sensitive to three particular decision parameters: solvent composition ($F_{propane}$) and duration of solvent injection in each cycle during the early SAS (T_{early}) and late SAS (T_{late}) stages. The decision variable vector **x** for this study is shown in Eq. 4.1:

$$\mathbf{x} = \{x_1, x_2, x_3\} = \{F_{propane}, T_{early}, T_{late}\} \quad \text{.....(4.1)}$$

where x_1, x_2, and x_3 refers to the three optimization parameters of $F_{propane}$, T_{early}, and T_{late}, respectively. Other variables, such as the methane concentration and duration of steam injection in each cycle, are dependent on the three selected decision variables and, hence, are not included in **x**.

Two options for formulating the MOO problem are examined in this study: a two-objectives optimization problem (Eq. 4.2) and a three-objectives optimization problem (Eq. 4.3). The objective vector **f**(**x**) for both options are defined as follow:

$$\mathbf{f}(\mathbf{x}) = \{f_1(\mathbf{x}), f_2(\mathbf{x})\} = \{cSOR,\ Propane_{retention}\} \quad \text{.....(4.2)}$$

$$\mathbf{f}(\mathbf{x}) = \{f_1(\mathbf{x}), f_2(\mathbf{x}), f_3(\mathbf{x})\} = \left\{Q_{propane},\ Q_{water},\ \frac{1}{RF}\right\} \quad \text{.....(4.3)}$$

where $cSOR$ is the cumulative steam-oil ratio and propane retention ($Propane_{retention}$) is the normalized volume of propane accumulated in the reservoir (Eq. 4.4). $Q_{propane}$ represents the cumulative injected propane volume, and it is normalized on a scale of 1 to 3 according to Eq. 4.5. Q_{water} denotes the cumulative injected steam volume, and it is normalized in a similar fashion as in Eq. 4.5. RF is recovery factor, which is the volume of cumulative oil production divided by the original oil in place, and 1/RF is used to transform this objective function for a minimization problem. It should be noted that all volumes mentioned here refer to their values at standard conditions.

$$Propane_{retention} = \frac{V_{propane}^{inj} - V_{propane}^{prod}}{V_{propane\_max}^{inj}} \quad \text{.....(4.4)}$$

$$Q_{propane} = \frac{Q_{propane}^{original} - Q_{propane\_min}^{original}}{Q_{propane\_max}^{original} - Q_{propane\_min}^{original}} \quad \text{.....(4.5)}$$

where $V_{propane}^{inj}$ and $V_{propane}^{prod}$ are the volumes of injected and produced propane, respectively, and $V_{propane\_max}^{inj}$ is the maximum volume of propane injected among all 144 cases of the

training dataset. $Q_{propane}^{original}$ is the cumulative solvent injection, and $Q_{propane\_min}^{original}$ and $Q_{propane\_max}^{original}$ are the lower and upper limits for the cumulative solvent injection. An initial set of 144 cases are generated for the proxy modeling step. Table 4.1 summarizes the ranges for each objective function corresponding to these 144 cases.

Table 4.1—Summary of the objective functions corresponding to the initial set of 144 SAS cases used for proxy modeling.

Parameter	Minimum	Maximum
cSOR (m^3/m^3)	2.17	2.44
$Propane_{retention}$	0.36	2.49
$Q_{propane}$ (m^3)	829070	6605000
Q_{water} (m^3)	168450	229370
RF (%)	44.14	55.34

4.2 Fundamentals of MOO

The idea of MOO is to minimize or maximize a number of objective functions, while ensuring that a number of different constraints are satisfied. The general form of a MOO problem is expressed as follow:

$$\left.\begin{array}{ll} f_m(\mathbf{x}), & m=1,2,...,M; \\ g_j(\mathbf{x}) \geq 0, & j=1,2,...,J; \\ h_k(\mathbf{x}) = 0, & k=1,2,...,K; \\ x_i^{(L)} \leq x_i \leq x_i^{(U)}, & i=1,2,...,n; \end{array}\right\} \quad \text{.....(4.6)}$$

$\mathbf{x}$ is a solution vector of n decision variables: $\mathbf{x} = (x_1, x_2, ..., x_n)^T$. The last sets of constraints are the variable bounds, restricting that each decision variable x_i to take a value between

the lower $x_i^{(L)}$ and upper $x_i^{(U)}$ bounds that constitute the decision space. For the sake of generality, there can be a total of J inequality statements and K equality constraints; the terms $g_j(\mathbf{x})$ and $h_k(\mathbf{x})$ are referred to as the constraint functions.

The two primary goals in solving a MOO problem are: (1) to find a set of non-dominated solutions, known as Pareto-optimal front, and (2) to search a set of solutions that are as diverse as possible. Pareto-optimality refers to an optimal allocation of resources (Min et al., 2014). It is mathematically defined as the condition of most non-domination. Non-domination is a state of equivalence, where no solution can be improved with respect to any objective function without worsening at least one other objective function (Srinivas et.al., 1994). Hence, it is essential when formulating a non-dominated sorting algorithm that all objective functions are equivalently important. A variable vector $\mathbf{x^1}$ is said to dominate another variable vector $\mathbf{x^2}$, if and only if Eq. 4.7 is satisfied:

$$\begin{aligned} &\forall i \in \{1,...,M\} : f_i\left(\mathbf{x^1}\right) \le f_i\left(\mathbf{x^2}\right) \\ &\text{and} \\ &\exists i \in \{1,...,M\} : f_i\left(\mathbf{x^1}\right) < f_i\left(\mathbf{x^2}\right) \end{aligned} \quad \text{..... (4.7)}$$

where the dominance of $\mathbf{x^1}$ over $\mathbf{x^2}$ is denoted as $\mathbf{f}\left(\mathbf{x^1}\right) \prec$ (Min et. al., 2017). The solutions would not only be converging along the Pareto-optimal front, but they should also be sparsely spaced in the Pareto-optimal region to ensure diversity and achieving a reasonable set of trade-off solutions based on the multiple objectives.

4.3 Non-dominated sorting genetic algorithm-II (NSGA-II)

In this study, NSGA-II (Deb et. al., 2002) is applied as a multi-objective optimizer to search for the Pareto-optimal solutions. This evolutionary algorithm alleviates the computational complexity of the original NSGA scheme, while presenting a fast non-dominated sorting approach for obtaining the Pareto-optimal set. Diversity preservation is applied to maintain a decent spread among the solution set.

The NSGA-II scheme can be summarized into the following steps: first, the parent population and the offspring population from the previous iteration are sorted into multiple fronts, such that the first front contains solutions that are completely non-dominant, and the second front contains solutions that are dominated only by the first front, and so on (Deb, 2001). Second, the new population is filled with the non-dominated solution from the first front. Third, if the size of new population is greater than the number of solutions from the first front, other non-dominated solution from the second front are added to the new population. Fourth, the filling process is repeated until the new population is filled and the current front is denoted as fr_m. Finally, the crowding distance is calculated for the solutions at the front fr_m, and those solutions with small average crowding distances are removed. The crowding distance (Eq. 4.8) (Deb, 2001) is a measure of how close an individual solution is to its neighbors; a large average crowding distance is preferred to ensure diversity in the new population.

$$\psi^j = \sum_{i=1}^{M} \frac{d_i^j}{f_i^{\max} - f_i^{\min}} \forall j = 1 : N_k \quad \text{.....(4.8)}$$

where ψ^j is the average crowding distance (over all M objective functions) for the j^{th} solution, d_i^j is the distance (difference in objective function f_i) between two neighboring solutions near the j^{th} solution along the axis of f_i, $f_i^{\max}$ and $f_i^{\min}$ are the maximum and minimum values of f_i, and N_k is the number of solutions in the k^{th} non-dominated front. The new population is used to generate a set of offspring using various crossover and mutation operators. This process is repeated for many iterations until a certain stop criterion (e.g., maximum number of generations) is met. Table 3 presents the optimization settings for the NSGA-II implementation for this study.

Table 4.2—NSGA-II settings.

Parameter	Value
Number of generations	100
Population size	200
Distribution index for crossover	20
Probability of mutation	0.33

4.4 Construction of Proxy Models: Response Surface Method

The response surface method (RSM) is used to approximate the relationships between the decision parameters and the objective functions via regression. A second-order (quadratic) non-linear model, as shown in Eq. 4.9, is employed:

$$f_i(\mathbf{x}) = \beta_0 + \beta_1 x_1 + \cdots + \beta_n x_n + \sum_{i=1}^{n} \beta_{ii} x_i^2 + \sum_{i<j} \sum_{i=2}^{n} \beta_{ij} x_i x_j + \varepsilon \quad \text{.....(4.9)}$$

where $f_i(\mathbf{x})$ is the objective function, and x_i is one of the n decision variables. The regression coefficients (β's) and the error term (ε) are adjusted during the calibration process. During a sensitivity analysis, the appropriate ranges of each decision variable are tested, and they are summarized in Table 4.3. As a result, a total of 9 × 4 × 4 = 144 cases are generated and subjected to flow simulations; their results are used for the training of two RSM models corresponding to the two objective functions in Eq. 4.2 or three RSM models corresponding to the three objective functions in Eq. 4.3.

Table 4.3—Experimental design: ranges and step sizes of the decision variables for proxy modeling.

	Lower Limit	Upper Limit	Step Size	Number of Steps
$F_{propane}$ (fraction)	0.5	0.9	0.05	9
T_{early} (months)	1	4	1	4
T_{late} (months)	1	4	1	4

4.5 Results and Discussion

4.5.1 Response Surface (Proxy) Modeling

The performances of the response surface proxy models are assessed by comparing the RSM predictions with the actual objective function values calculated from flow simulation results for the 144 SAS scenarios. The comparisons are shown in Figure 4.1, and since the coefficients of determination (R^2) are greater than 0.85 for all objective

functions, it is concluded that the trained RSM models can be used to approximate the objective functions in the optimization step.

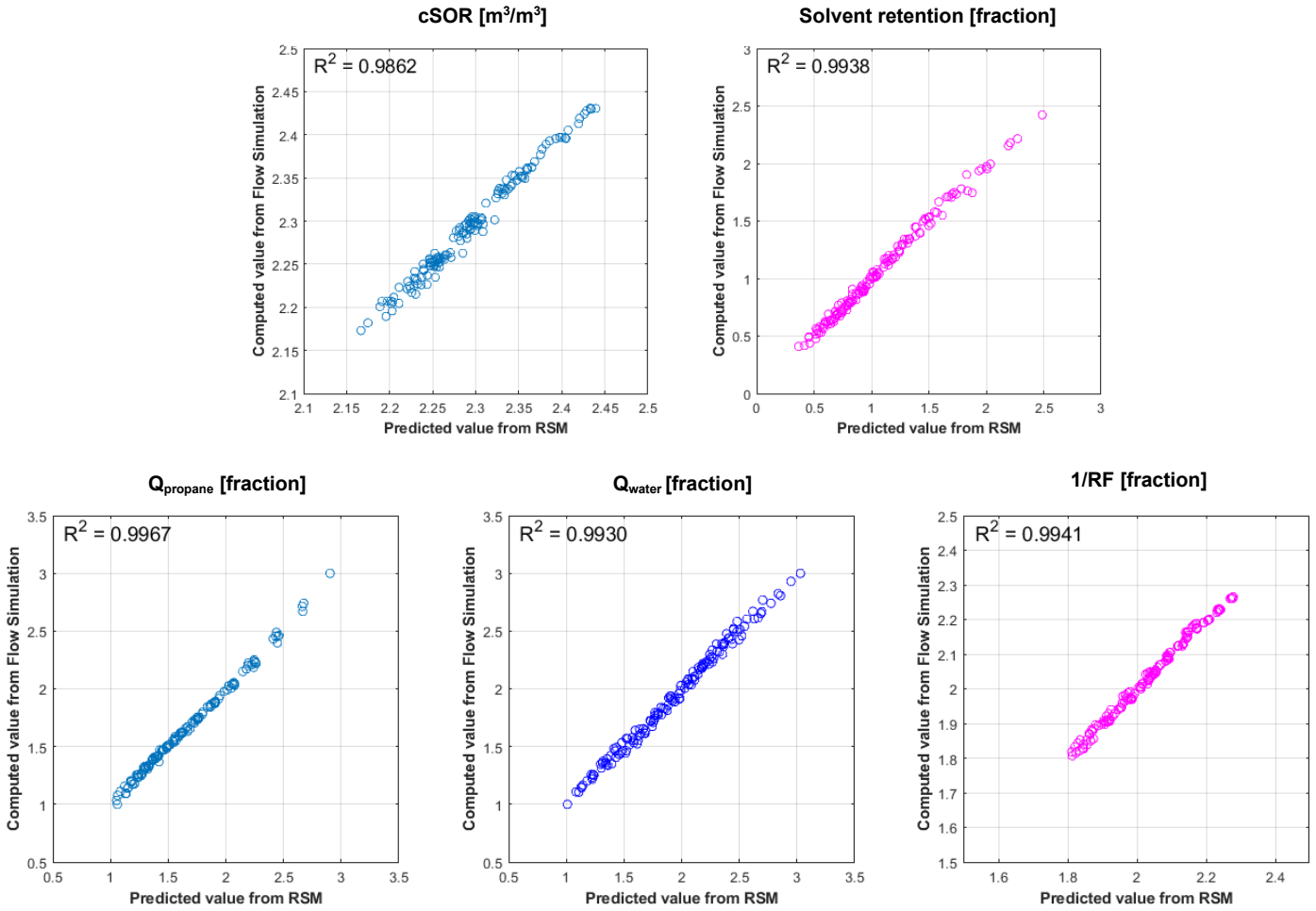

Figure 4.1—Comparison between the flow simulation data and the predicted values from RSM proxy model: top row: two objective functions; bottom row: three objective functions.

4.5.2 Optimization Results and Discussions

4.5.2.1 Two-objectives optimization

The Pareto-optimal front for the SAS process is presented in Figure 4.2. Two regions can be identified: (a) and (b). The initial and final ranges of the decision variables and the corresponding objective functions are summarized in Tables 4.4 and 4.5, respectively.

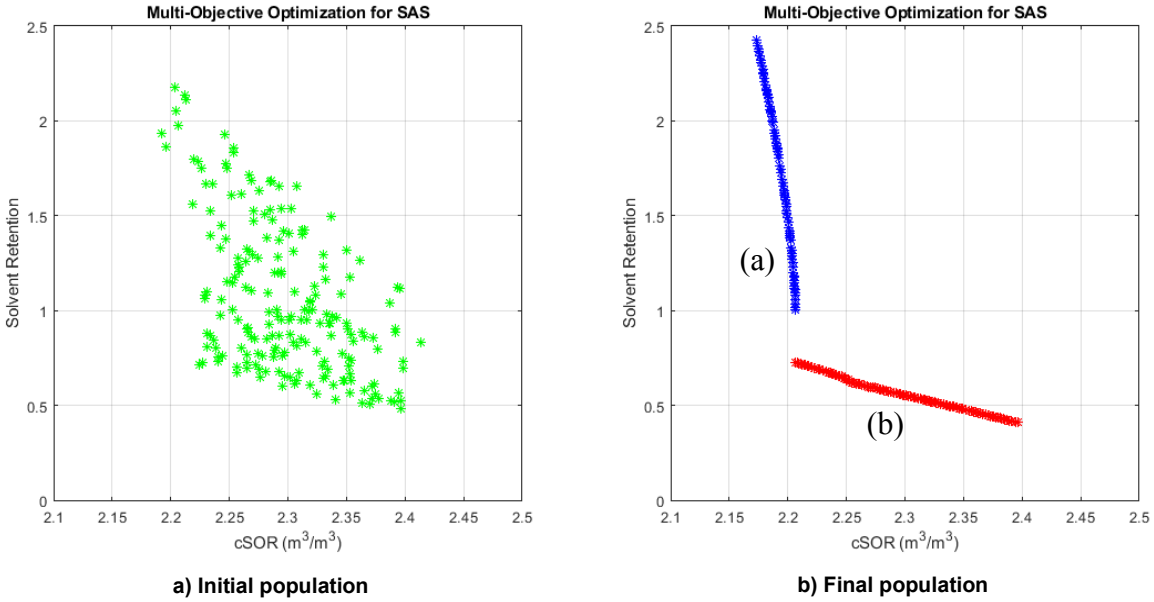

a) Initial population **b) Final population**

Figure 4.2—Pareto-optimal front for the SAS process: a) first iteration; b) last iteration: blue – region (a); red – region (b).

It is observed that 45% of the cases along the Pareto front would belong to region (a), while the remaining 55% resides in region (b). The decision parameter ranges for region (a) correspond to an operational strategy involving prolonged periods of solvent injection in both the early and late SAS cycles, with the propane fraction varying anywhere between 0.59 and 0.90 (the maximum value). Generally, the cases in region (a) exhibit

lower *cSOR* values because the duration for steam injection in each cycle is shorter. On the other hand, the decision parameter ranges for region (b) reflect an operational strategy where solvent injection is minimized (i.e., lowest allowable level for the propane fraction); slightly longer solvent injection durations can be employed during the early cycles, but shorter solvent injection durations are clearly preferred during the late cycles (Figure 4.3).

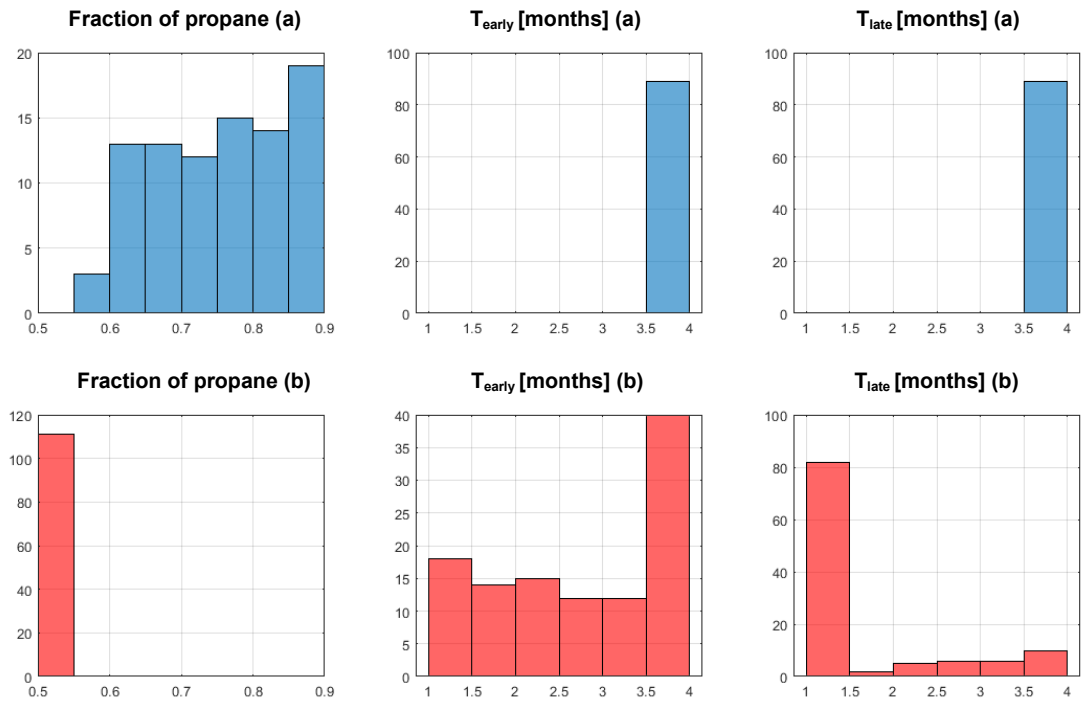

Figure 4.3—Histograms of decision parameters: blue – region (a); red – region (b).

Table 4.4—Initial ranges of decision parameters and objective functions prior to optimization.

cSOR ***(m^3/m^3)***	***$Propane_{retention}$*** ***normalized***	***$F_{propane}$***	***T_{early}*** (months)	***T_{late}*** (months)
[2.17, 2.44]	[0.36, 2.49]	[0.5, 0.9]	[1, 4]	[1, 4]

Table 4.5—Final ranges of decision parameters and objective functions after optimization.

Number of results	***cSOR (m^3/m^3)***	***$Propane_{retention}$ normalized***	***$F_{propane}$***	***T_{early}*** (months)	***T_{late}*** (months)
a - 89	[2.14, 2.30]	[0.53, 2.17]	[0.59, 0.90]	[4]	[4]
b - 111	[2.37, 2.42]	[0.46, 0.53]	[0.50, 0.51]	[1, 4]	[1, 4]

There is a noticeable gap in the front right between regions (a) and (b). The two points on either ends of the gap (one from each region). The solvent injection durations are at the maximum value for both points. However, the difference in propane concentration has contributed to the gap: lower fraction of propane has resulted in lower propane retention, which represents with 0.50 fraction of propane we have 0.73 normalized propane retention, and with 0.59 fraction of propane the normalized propane retention is 1.00, having the same *cSOR* in both cases (with 2 months of steam injection in each cycle).

The results of these two regions highlight the trade-off between the two objective functions: solvent retention and *cSOR*. If we isolate a set of 93 "most optimal" results along the Pareto front, as marked in red in Figure 4.4, and analyze their decision parameters (Table 4.6), it can be concluded that the most optimal scheme is to inject a solvent with lower propane concentration for a longer duration during the early cycles, although the injection duration can be increased during the late cycles.

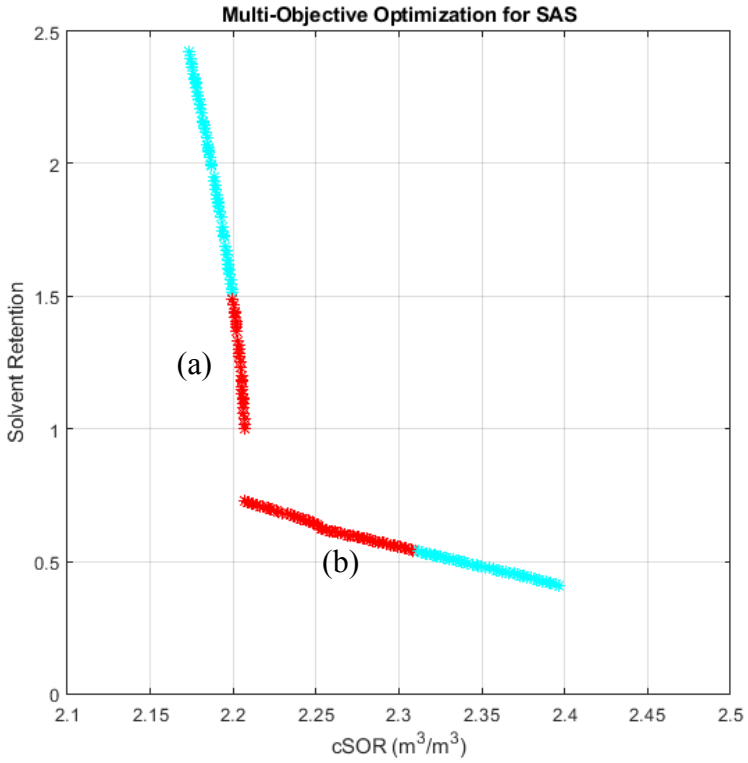

Figure 4.4— Selected cases (red) along the Pareto-optimal front for the SAS process.

Table 4.6—Proposed ranges of decision parameters and objective functions after optimization.

Number of results	***cSOR (m^3/m^3)***	***$Propane_{retention}$ normalized***	***$F_{propane}$***	***T_{early}*** (months)	***T_{late}*** (months)
93	[2.20, 2.31]	[0.54, 1.49]	[0.50, 0.71]	[2.64, 4]	[1, 4]

Looking specifically at histograms of the optimization parameters of the red front in the two regions (Figure 4.5), (a) suggests that the solvent should be injected at 4 months per cycle in the early and late stage, having a concentration of propane between 0.6 and 0.7. However, region (b) shows that it is also optimum if the operation consists in injecting low concentration of propane the longer time possible in the early cycles of SAS, but changing to shorter periods of solvent injection in the late cycles of SAS.

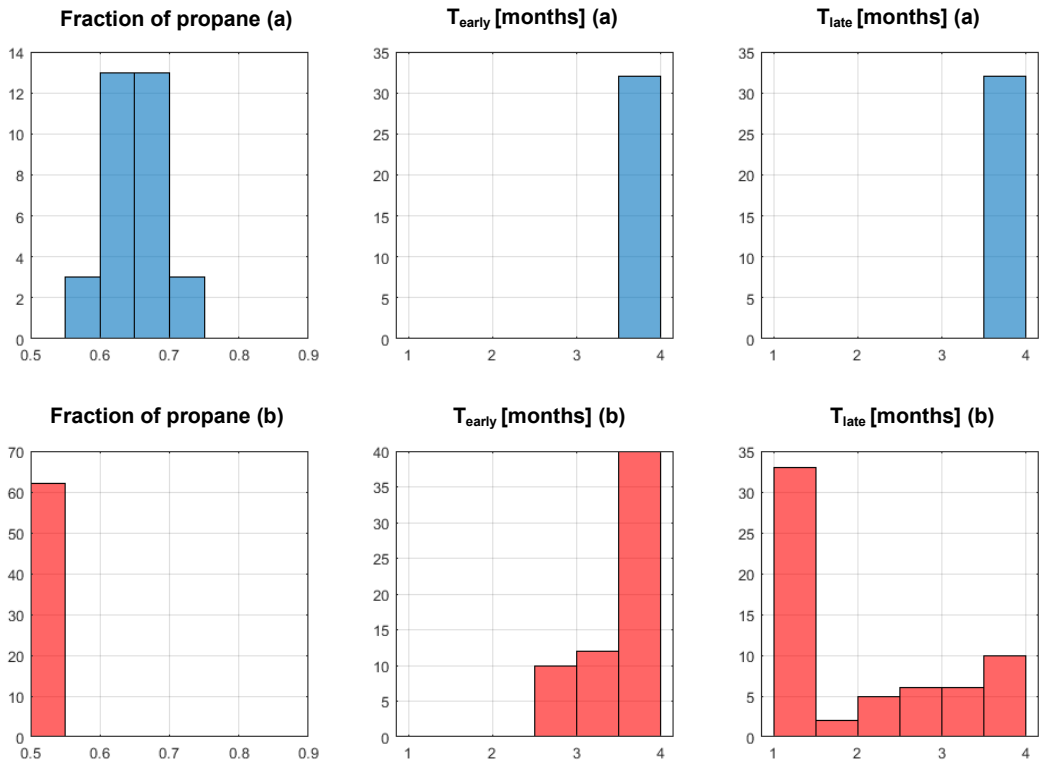

Figure 4.5— Histograms of decision parameters of the 93 "most optimal" results: blue – region (a); red – region (b).

4.5.2.2 Three-objectives optimization

For three objective functions, the optimization results in a three-dimensional space is shown in Figure 4.6. It is noted that as the iteration progresses, the Pareto front tends to advance towards the outer limits/boundaries of the initial population. Similar to the two-objectives problem, three distinct clusters of solutions can be identified from the final Pareto-optimal set. These clusters reflect the trade-off among these conflicting objectives – in each cluster, one of the three objectives is penalized, while the other two are minimized. For each objective function (expressed in fractions), the mid-point between its maximum and minimum values is used to define the three clusters (or regions) as follow:

- Region (a) [71 cases] – Q_{water} < average; RF < average, $Q_{propane}$ < average for 65 out of the 71 cases. This cluster corresponds to an operational scenario where little steam and solvent are injected (minimizing 2/3 of the objective functions), despite of the low oil production.
- Region (b) [51 cases] – $Q_{propane}$ < average; RF > average; Q_{water} > average. This cluster corresponds to an operational scenario where low volumes of solvent are needed for the high oil production (minimizing 2/3 of the objective functions), despite of the high steam injected volumes.
- Region (c) [72 cases] – $Q_{propane}$ > average; RF > average; There is slightly more scattering in the ranges for Q_{water}: for most of the solutions, Q_{water} is close to the average (Figure 4.7 ii).

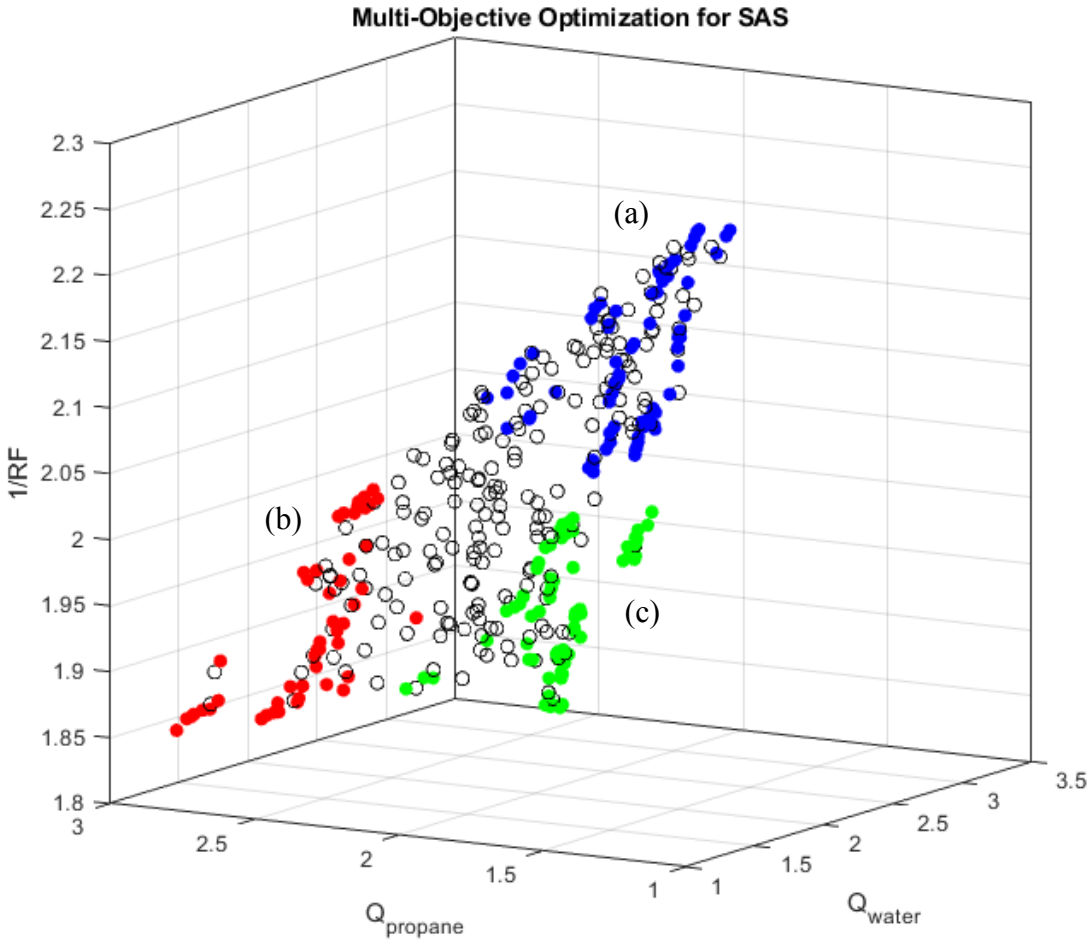

Figure 4.6—Pareto-optimal front for the SAS process: black circles – initial population, colored circles – final population: blue – region (a); red – region (b); green – region (c).

The results illustrate that when the three objective functions are highly correlated with one another, and the trade-off among them becomes very evident during the MOO optimization. For example, less solvent is needed if the steam injection is prolonged, and vice versa. Each set of solutions, i.e., regions (a), (b), or (c), is optimized in terms of two of the objective functions. It is essentially impossible to minimize all three objective functions simultaneously. Therefore, the MOO method attempts to identify a set of possible scenarios that would minimize these objective functions to various extent. Figure 4.7 shows the projections of the 3D Pareto optimal surface onto a set of 2D spaces. Region (a)

corresponds to the situation with the low Q_{water} and $Q_{propane}$ (subplot iii); region (b) corresponds to the cases with low $Q_{propane}$ and 1/RF (subplot i). Finally, for region (c), both Q_{water} and1/RF are low (subplot ii), despite that the solutions are more scattered along the front, in comparison to the other two regions. Specifically, for this region, most of the values of Q_{water} are close to their average, some of them are just slightly higher than the average.

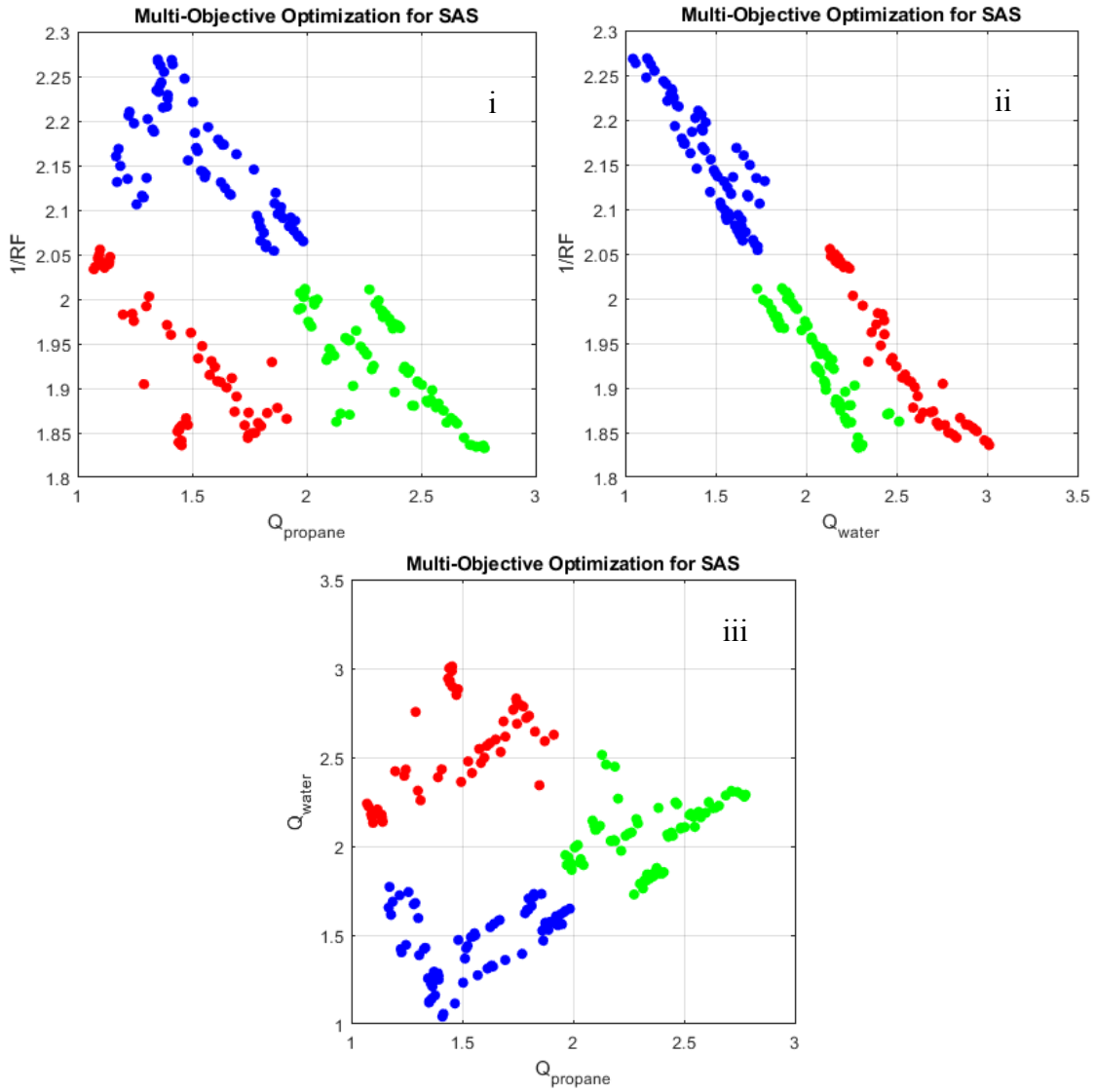

Figure 4.7—Projections of the Pareto-optimal front for the SAS process onto three 2D planes for the final population: i) 1/RF vs $Q_{propane}$; ii) 1/RF vs Q_{water} iii) Q_{water} vs $Q_{propane}$ [blue – region (a); red – region (b); green – region (c)].

The distributions of the optimal decision parameters for the various regions are presented in Figure 4.8. For region (a), the process should be operated by injecting solvent mixtures with low concentrations of propane for longer periods of time during both the early and late stages, such that the steam injection requirement is also reduced. For region (b), to maximize recovery while reducing the solvent requirement, it is recommended to inject solvent mixtures with high concentration of propane for shorter periods of time during both the early and late stages. For region (c), to maximize recovery while reducing the steam requirement, it is recommended to inject solvent mixtures with high concentration of propane for long periods of time.

If the histograms in Figure 4.8 (three objective functions) are compared to those in Figure 4.5 (two objective functions), the following inferences can be made:

- Region (a) in Figure 4.5 and region (c) in Figure 4.8 are similar – injecting higher concentration of propane for longer periods of time.
- Region (b) in Figure 4.5 and region (a) in Figure 4.8 are similar – injecting lower concentration of propane for longer periods of time.

It is reasonable to obtain different solutions, depending on the objective function formulation. For example, the solutions in region (b) in Figure 4.5 are not directly identifiable from the two-objectives optimization because Q_{water} and $1/RF$ are combined into a single objective function of *cSOR*. It should be recalled that region (b) corresponds to a situation with prolonged periods of steam injection, and this choice is unlikely to be located along the Pareto front, if *cSOR* is considered as one of the two objective functions.

It has been concluded previously (based on the most optimal cases from the two-objectives optimization) that the most optimal scheme is to inject a solvent with lower propane concentration for longer durations, especially for the early cycles. This conclusion still holds with respect to the three-objectives optimization analysis. However, the three-objectives results seem to identify an additional option in accordance to region (b), where solvents with high propane concentration is injected for shorter durations (maximizing oil recovery while minimizing solvent requirement). Therefore, considering both sets of MOO results, the following is recommended: (1) if steam availability or consumption is to be limited, one should inject solvents with low concentration of propane for the maximum duration; (2) otherwise, one should inject solvents with high concentration of propane for a short period, followed by steam injection.

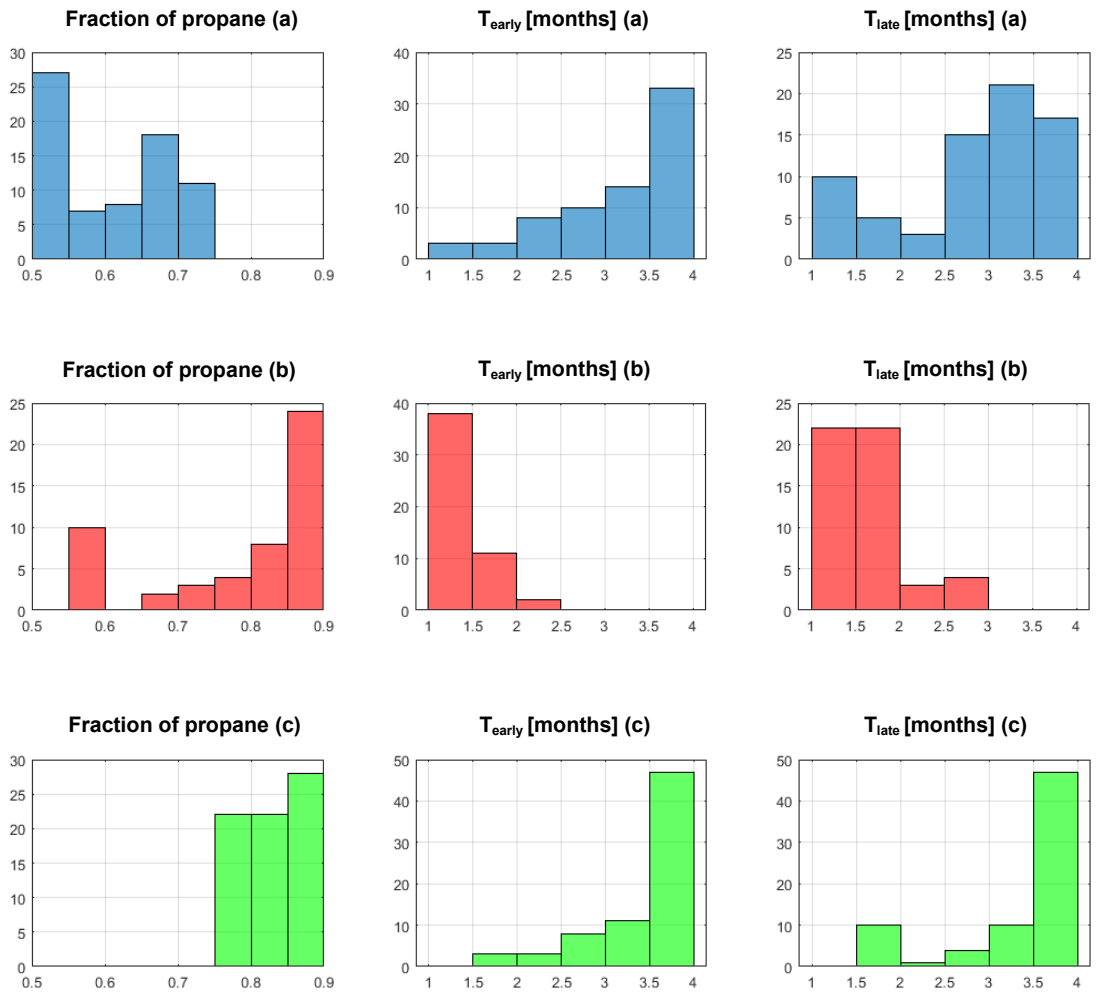

Figure 4.8— Histograms of decision parameters: blue – region (a); red – region (b); green – region (c).

Table 4.7—Final ranges of decision parameters after optimization (3 objective functions).

Number of results	$F_{propane}$	T_{early} (months)	T_{late} (months)
a - 71	[0.50, 0.72]	[1.39, 4.00]	[1.07, 3.93]
b - 51	[0.58, 0.90]	[1.00, 2.47]	[1.06, 2.57]
c - 72	[0.76, 0.90]	[1.70, 4.00]	[1.69, 3.99]

In terms of economics of the process, the energy input per unit oil produced should be consider for accurate calculations. For this study, the advantage of an optimized

operation is compared to the base case. The cost of the solvent varies, and it is not considered, and the comparison will be in terms of the volumes of injected solvent required and the oil recovered. The base case is operated at 4-months injection of solvent in the early and late stages of the SAS process with 0.8 of fraction of propane in the solvent mixture. An optimal case from the 2-objective functions approach is chosen, with a duration of solvent injection of 4-months in the early SAS stage and 1-month in the late SAS, with a fraction of propane of 0.5 in the solvent mixture. Both cases have a similar value of *cSOR*, 2.20 in the base case and 2.25 in the optimized case, but the optimal case has a 0.62 [fraction] of propane retention compared to the 1.82 of the base case (this value being normalized between 0.36 and 2.49). The cumulative oil produced in the base case was 88018 m^3, higher compared to the optimal case, which produced 77038 m^3 of oil, with a difference of approximately 11000 m^3. In terms of the propane requirement, for the base case, 4.87×10^6 m^3 solvent is injected and 3.35×10^6 m^3 produced, with 1.52×10^6 m^3 of propane retained in the reservoir, but for the chosen optimal case, 1.51×10^6 m^3 of propane is required and 1.02×10^6 m^3 is produced, representing a 0.49×10^6 m^3 of propane retention. The difference in solvent retention between the two sets of operational parameters is 1.02×10^6 m^3 of propane. Since the *cSOR* is similar in both cases, it is important to compare their corresponding ratios of the oil produced and propane retention. For the base case, 0.058 m^3 of oil is produced per m^3 of propane retained, while for the optimal case, 0.157 m^3 of oil is produced per m^3 of propane retained. Therefore, it is concluded that the optimal case would yield better project economics than the base case, especially when the costs of GHG emissions (e.g, carbon tax, social license for oil and gas operations) are considered.

Another advantage of the proposed hybrid optimization workflow is the considerable savings in computational costs. For instance, a single simulation run takes approximately 7 minutes, while estimating the objective function value using the response surface models would take less than a second. It should be noted that a limited number of initial models are required to build the proxy models, and this front-end loading in computational costs can be justified given that it takes approximately one minute using a personal computer [Intel(R) Core (TM) i7-3770 CPU (3.40 GHz) and 16 GB of installed memory (RAM)] to obtain a set of Pareto-optimal solutions from an initial population of 200. In contrast, if the full flow simulation is implemented, it would take 97 days [100 iterations $\times$ 200 simulation runs per iteration $\times$ 7 minutes/simulation run] to complete all the calculations without any parallel computation. There is a significant improvement in terms of computational efficiency.

Chapter 5 Design of Steam Alternating Solvent Process Operational Parameters Considering Shale Heterogeneity

5.1 Selection of Decision Parameters and Objective Functions

A similar sensitivity analysis procedure, as applied in Coimbra et al., (2019), is used here to formulate the decision variables and objective functions for the design of SAS process in heterogeneous reservoirs. The SAS performance is primarily sensitive to three particular decision parameters: solvent composition ($F_{propane}$) and duration of solvent injection in each cycle during the early SAS (T_{early}) and late SAS (T_{late}) stages. To account for the trade-off between oil production, solvent retention, and steam injection, two objective functions: (1) cumulative steam-oil ratio, *cSOR* [m^3/m^3] and (2) propane retention ($Propane_{retention}$) [fraction] are formulated as follows:

$$\mathbf{f}(\mathbf{x}) = \{f_1(\mathbf{x}), f_2(\mathbf{x})\} = \{cSOR,\ Propane_{retention}\} \quad \text{.....(5.1)}$$

where **x** denotes the decision variable vector consisting of $F_{propane}$, T_{early}, and T_{late}, and **f** is the objective function vector. Propane retention is defined as the difference between the volume of propane injected and the volume of propane produced, normalized based on the lowest possible propane injection volume among the entire training data set for the response surface modeling, as shown in Eq. 5.2:

$$Propane_{retention} = \frac{V_{propane}^{inj} - V_{propane}^{prod}}{V_{propane\_max}^{inj}} \quad \text{.....(5.2)}$$

where $V_{propane}^{inj}$ and $V_{propane}^{prod}$ refers to the injected and produced propane volume at reservoir conditions [m^3] respectively. For normalization purposes, the retained volume is divided by $V_{propane\_max}^{inj}$, which is the maximum injected volume among all the cases in the initial training set for the RSM modeling.

For each objective function, an overall (aggregated) value encompassing all ten reservoir models will be computed using the mean, maximum and minimum values of the respective objective functions from all ten realizations. The ranges of the objective functions for one of the ten heterogeneous models are presented in Table 5.1.

Table 5.1—Summary of the objective functions corresponding to the initial set of 144 SAS cases of one randomly-selected heterogeneous reservoir used for proxy modeling.

Parameter	Minimum	Maximum
cSOR (m^3/m^3)	2.10	2.49
$Propane_{retention}$ normalized (fraction)	0.48	2.66
$Propane_{retention}$ in SI Units (m^3)	428240	2376200

5.2 Introduction of MOO and Non-Dominated Sorting Genetic Algorithm-II (NSGA-II)

The purpose of MOO is to minimize or maximize a number of objective functions, while ensuring that the set of solutions are satisfying a number of different constraints. This problem can be expressed mathematically as follows:

$$\left.\begin{array}{ll} f_m(\mathbf{x}), & m=1,2,...,M; \\ g_j(\mathbf{x}) \geq 0, & j=1,2,...,J; \\ h_k(\mathbf{x}) = 0, & k=1,2,...,K; \\ x_i^{(L)} \leq x_i \leq x_i^{(U)}, & i=1,2,...,n; \end{array}\right\} \quad \text{.....(5.3)}$$

where $\mathbf{x}$ represents a solution vector $\mathbf{x} = (x_1, x_2, ..., x_n)^T$ and each element in $\mathbf{x}$ denotes a decision variable [i.e., $F_{propane}$, T_{early}, T_{late}]. $g_j(\mathbf{x})$ and $h_k(\mathbf{x})$ are two different constraint functions. The lower and upper bounds for each decision variable i are defined by the last equation.

The problem is solved by (1) finding a set of non-dominated solutions that are as close as possible to the set of true optimal solutions, also known as the Pareto front and (2) maintaining diversity among the set of non-dominated solutions. Pareto-optimality refers to an optimization state when no solution can be enhanced in any objective function without compromising at least one other objective function (Deb, 2001). Readers should refer to the references for further discussions on the concept of non-dominance and other MOO implementations.

An elitist multi-objective evolutionary algorithm, NSGA-II, (Deb et al., 2002) is applied here. The principal characteristics of this scheme is that it uses an elite-preservation strategy (i.e., an operator that enables the elites of a given population to be directly carried over onto the next generation (Deb, 2001); in the meantime, an explicit diversity-preserving mechanism is in place to maintain a decent spread among the solution set. The key steps can be described as follow:

1. Sorting of solutions – The parent population and the offspring population from the previous iteration are sorted into multiple fronts in descending order of dominance: the completely non-dominant solutions are placed in the first front, and solutions that are dominated only by the first front are assigned in the second front (Deb, 2001).
2. Construction of the new population – The new population is first filled with all the solution from the first front. If there are insufficient solutions from the first front to fill the entire new population, other non-dominated solution from the second front are added. In fact, this filling process continues with adding more solutions from other fronts, until the entire new population is filled, and the current front is denoted as f_{rm}. A crowding distance is computed for all the solutions at front f_{rm}, and those solutions with the lowest average crowding distances are removed. The crowding distance (Eq. 5.4) (Deb, 2001) is a measure of how close an individual solution is to its neighbors; a large average crowding distance is preferred to ensure diversity in the new population. The idea is that when there are more solutions in f_{rm} than there are empty spots in the new population, it is better to select those that are more diverse, given that they are all equally optimal along the same front f_{rm}.

$$\psi^j = \sum_{i=1}^{M} \frac{d_i^j}{f_i^{\max} - f_i^{\min}} \forall j = 1 : N_k \quad \text{.....(5.4)}$$

For the j^{th} solution, ψ^j is the average crowding distance over all M objective functions; the distance d_i^j is computed as the difference in objective function f_i between two neighboring solutions near the j^{th} solution along the axis of f_i; the

maximum and minimum values of the objective function f_i are denoted by $f_i^{\max}$ and $f_i^{\min}$, respectively; N_k is the total number of solutions along the k^{th} non-dominated front.

3. Generation of new offspring – The new population is subjected to various crossover and mutation operators.
4. Steps 1-3 are repeated iteratively until a certain stop criterion (e.g., maximum number of generations) is achieved. The optimization settings implementation in this study is summarized in Table 5.2.

Table 5.2—NSGA-II configuration.

Setting	Value
Number of generations	100
Population size	200
Distribution index for crossover	20
Probability of mutation	0.33

5.3 Construction of Response Surface Proxy Models

The response surface method (RSM) is used to build a set of proxy models for full flow simulation to approximate the complex relationship between the three decision variables and two objective functions. Once calibrated, the response surface model, instead of the flow simulation, is used to estimate the objective functions directly, enhancing the computing efficiency of the MOO scheme. This work employs the interactive RSM toolbox in Matlab™ (MathWorks, 2019), which applies a second-order (quadratic) non-linear model as shown in Eq. 5.5:

$$f_i(\mathbf{x}) = \beta_0 + \beta_1 x_1 + \cdots + \beta_n x_n + \sum_{i=1}^{n} \beta_{ii} x_i^2 + \sum_{i<j} \sum_{i=2}^{n} \beta_{ij} x_i x_j + \varepsilon \quad \text{.....(5.5)}$$

where $f_i(\mathbf{x})$ is the objective function, x_i is the decision variable. The regression coefficients (β's) and the error term (ε) are adjusted during the calibration process.

The ranges of each decision variable proposed in this work are investigated during the sensitivity analysis. Ten sets of 144 SAS cases are generated (one set for each heterogeneous realization). Each decision variable is divided into different levels (steps), and a total of 9 × 4 × 4 = 144 cases are generated and subjected to flow simulations for each realization. The results of the flow simulation are used to compute the objective functions and to train two RSM models for each realization (i.e., 10 sets of RSM coefficients are obtained for each objective function per heterogeneous realization). The overall value is computed by aggregating the RSM model results for all ten realizations based on either the average, minimum, or maximum values.

Table 5.3—Experimental design: ranges and step sizes of the decision variables for proxy (RSM) modeling.

	Lower Limit	Upper Limit	Step Size	Number of Steps
$F_{propane}$ (fraction)	0.5	0.9	0.05	9
T_{early} (months)	1	4	1	4
T_{late} (months)	1	4	1	4

5.4 Proposed Hybrid MOO Workflow

The workflow for designing the SAS process considering reservoir heterogeneity is presented in Figure 5.1. The entire workflow consists of four main steps: (1) sensitivity

analysis is conducted to identify the appropriate decision parameters and the corresponding objective functions; (2) assembling a training dataset for the RSM modeling; (3) RSM proxy models are constructed; and (4) MOO is applied to compute the objective functions and the corresponding set of Pareto-optimal decision parameters.

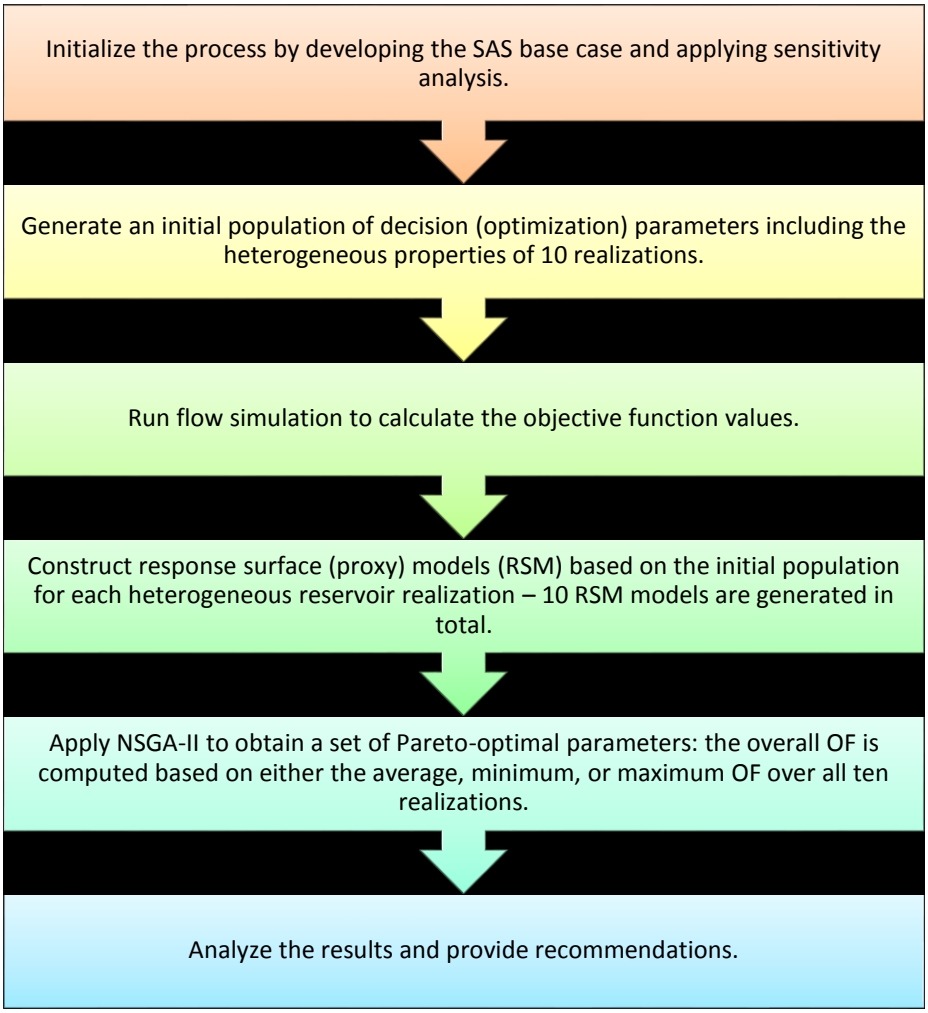

Figure 5.1—Flow diagram of the Hybrid SAS optimization process with the consideration of reservoir heterogeneity.

5.5 Results and Discussion

5.5.1 Response Surface (Proxy) Modeling

Figure 5.2 compares the RSM proxy predictions to the target values (actual flow simulation results) for one set of the 144 SAS cases used in the training step (there are 144 SAS cases for each heterogeneous realization). The results indicate that the trained RSM models can be used to reliably approximate the objective functions in the MOO scheme. The coefficients of determination (R^2) for all 10 heterogeneous realizations are summarized in Table 5.4, and all the values are greater than 0.95 for both objective functions.

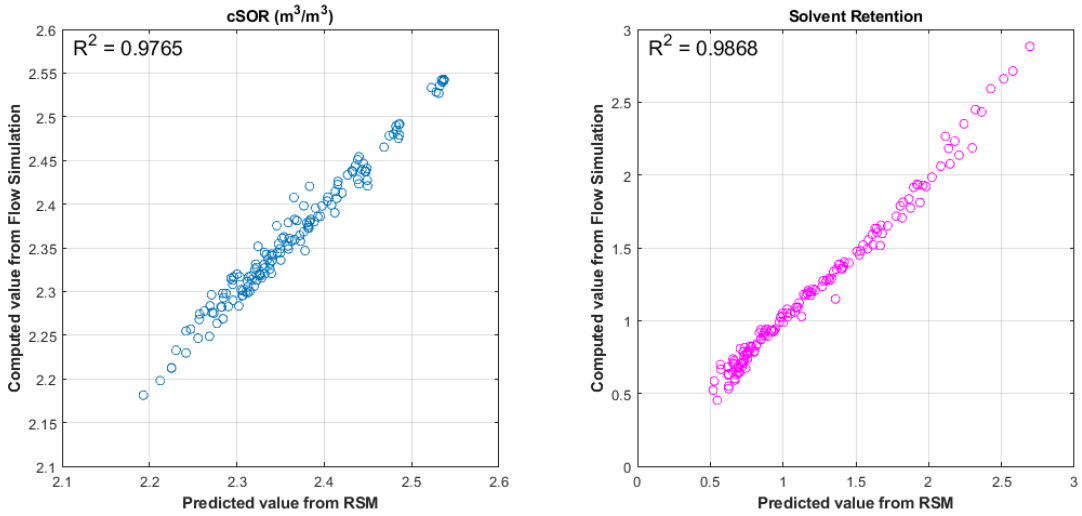

Figure 5.2—Comparison between the flow simulation data and the predicted values from RSM proxy model for one of the heterogeneous cases (case 5).

Table 5.4—Experimental design: ranges and step sizes of the decision variables for proxy (RSM) modeling.

Heterogeneous Realization	Coefficients of Determination (R^2) [fraction]	
	cSOR	***Propane (Solvent) Retention***
1	0.9922	0.9872
2	0.9561	0.9880
3	0.9778	0.9915
4	0.9491	0.9914
5	0.9765	0.9868
6	0.9792	0.9880
7	0.9908	0.9918
8	0.9868	0.9932
9	0.9823	0.9893
10	0.9931	0.9940

5.5.2 Optimization Results and Discussions

Three Pareto-optimal fronts for the SAS process in heterogeneous reservoirs are illustrated in Figure 5.3. The results indicate that the *cSOR* is more sensitive to the way the objective function is computed (i.e., average, minimum or maximum). The fronts can be divided into 2 regions (a) and (b). Each region represents a specific optimal combination of decision parameters (Table 5.5).

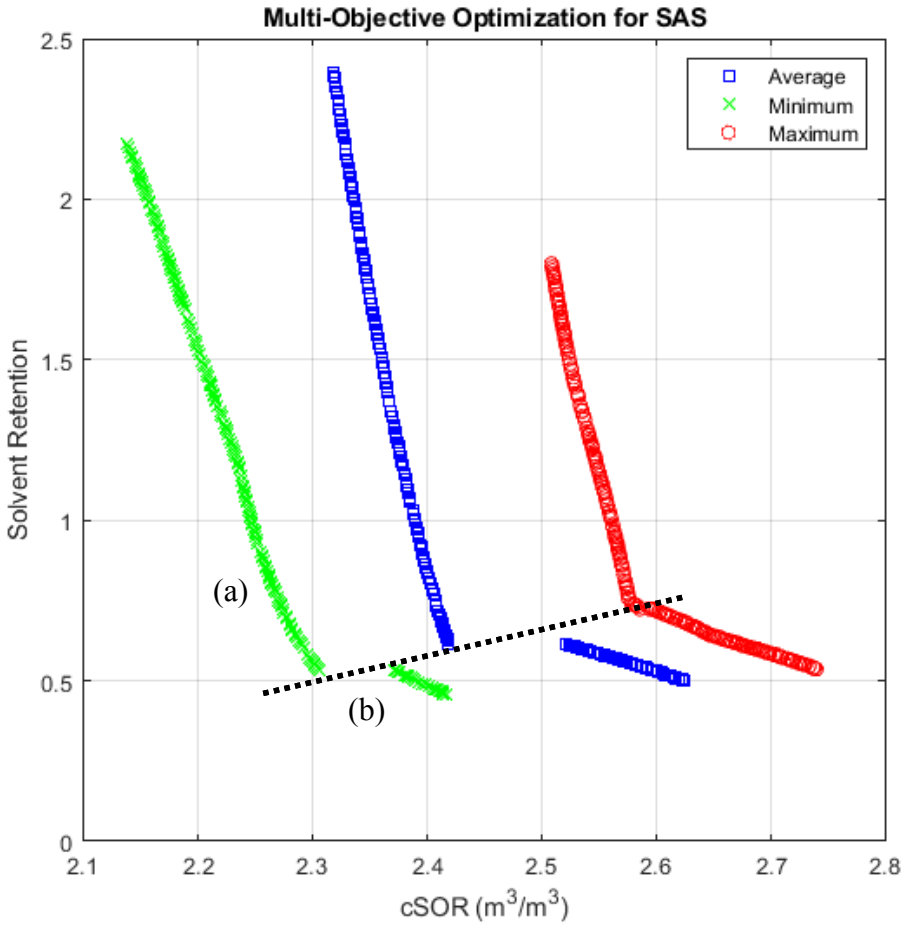

Figure 5.3—Pareto-optimal front for the SAS process for the last iteration corresponding to the three different overall objective function formulations.

Table 5.5—Final ranges of objective functions after optimization and decision parameters.

Case	Number of cases (population size = 200)	cSOR [m^3/m^3]	Solvent retention normalized	$F_{propane}$	T_{early} [months]	T_{late} [months]
Min	a - 171	[2.14, 2.30]	[0.53, 2.17]	[0.50, 0.90]	[3.60, 4]	[3.90, 4]
	b - 29	[2.37, 2.42]	[0.46, 0.53]	[0.50, 0.51]	[1, 1.69]	[1, 1.17]
Ave	a - 142	[2.31, 2.41]	[0.61, 2.39]	[0.50, 0.90]	[3.95, 4]	[3.94, 4]

	b - 58	[2.52, 2.62]	[0.49, 0.90]	[0.50, 0.53]	[1, 2.22]	[1, 1.07]
Max	a - 111	[2.51, 2.58]	[0.74, 1.80]	[0.50, 0.78]	[3.92, 4]	[1, 4]
	b - 85	[2.59, 2.74]	[0.54, 0.72]	[0.50, 0.54]	[1, 3.44]	[1, 1.09]

Among the 200 results, region (a) encompasses the most of the optimal cases, irrespective to how the overall objective function is assessed. If it is based on the minimum value, 85.5% of the cases along the Pareto front would belong to region (a); for the average and maximum values, 71% and 56% of the optimal cases would belong to region (a), respectively.

Figure 5.4 illustrates the specific sets of optimal parameters for each region when the overall objective function is computed as the average among all 10 heterogeneous realizations. The optimal parameters from region (a) point to a conclusion that the process should be operated with longer periods of solvent injection during each 6-month cycle [i.e., 3.94 – 4 months, which is the pre-defined maximum allowable value], and the corresponding fraction of propane may vary from 0.5 to 0.9. The region of lower solvent retention and lower *cSOR* corresponds to long periods of solvent injection in the early and late times, along with low propane concentration (close to the predefined lower bound value of 0.5). On the other hand, region (b) represents the scenario where the least amount of solvent is injected: low fraction of propane in the solvent injected over a short duration during both early and late cycles.

The results corresponding to these two regions clearly illustrate the trade-off between the two objective functions: solvent retention and *cSOR*. For region (a), more

solvent is injected (long periods of injection in both early and late cycles) leads to high recovery and low steam injection (i.e., low *cSOR*). Given that the duration of every cycle is fixed as 6 months, a longer solvent injection period must be accompanied by a shorter steam injection period. The obvious trade-off is that there is likely to be high solvent retention. In contrast, for region (b), very little solvent is injected, so solvent retention is low; however, steam is injected during much of each cycle, which leads to high *cSOR*.

Same conclusions can be drawn if the overall objective function is computed based on the minimum among all 10 heterogeneous realizations (Figure 5.5). The difference, however, is the position of the front, as it is shifted to the left. This is because the minimum value for the objective of *cSOR* is usually less than the average value, while the optimal solvent retention values are not overly sensitive to how this objective function is being aggregated.

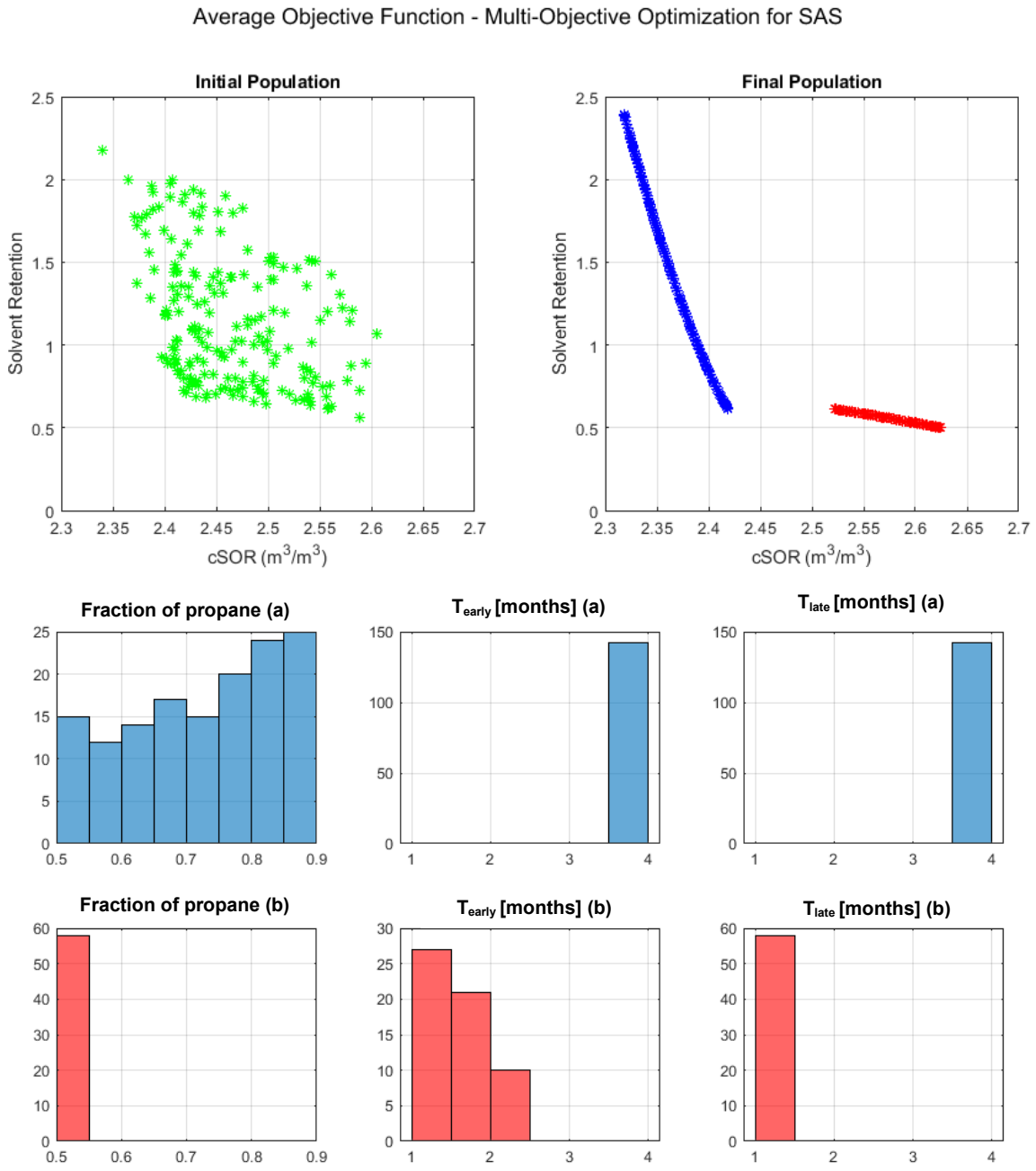

Figure 5.4—Pareto-front and histograms of decision parameters when the overall objective function is computed as the average among all 10 heterogeneous realizations: blue – region (a); red – region (b).

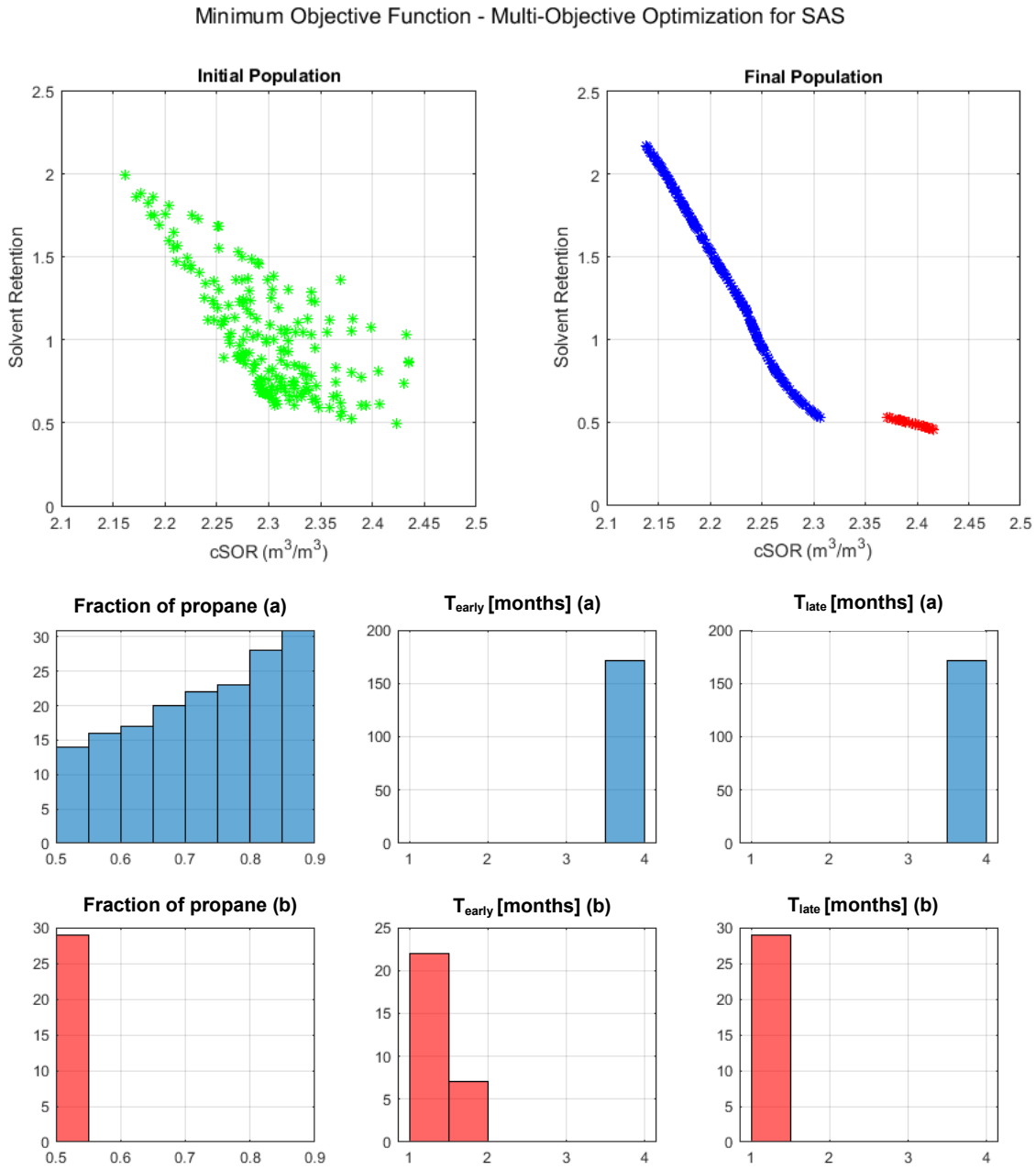

Figure 5.5—Pareto-front and histograms of decision parameters when the overall objective function is computed as the minimum among all 10 heterogeneous realizations: blue – region (a); red – region (b).

When the overall value is computed based on the maximum among all ten realizations, a new cluster of cases seems to emerge (they are marked as green in Fig. 5.6) – they differ from the two aforementioned groups and are, in fact, located in between those

two groups in the objective function cross plot. In comparison to the other cases in region (b), this new cluster of cases seems to recommend a slightly longer solvent injection duration for the early times. A plausible explanation is that the maximum objective function values are typically associated with the most heterogeneous cases (e.g., one with many shale barriers, possibly in the near-well region); in such cases, it may be necessary to prolong the solvent injection period. Interestingly, extending the solvent injection duration for the late times does not seem to improve the objective functions significantly. It is observed for region (a), solutions along the Pareto front exhibit lower solvent retention. Inspecting the histograms in Fig. 14 reveals that less solvent is generally injected when the maximum objective function values are considered. Once again, as the maximum objective function values often correspond to the most heterogeneous cases, where the solvent chamber development is impeded and less oil is produced; given that the injector is pressure constrained, less solvent could be injected in such cases.

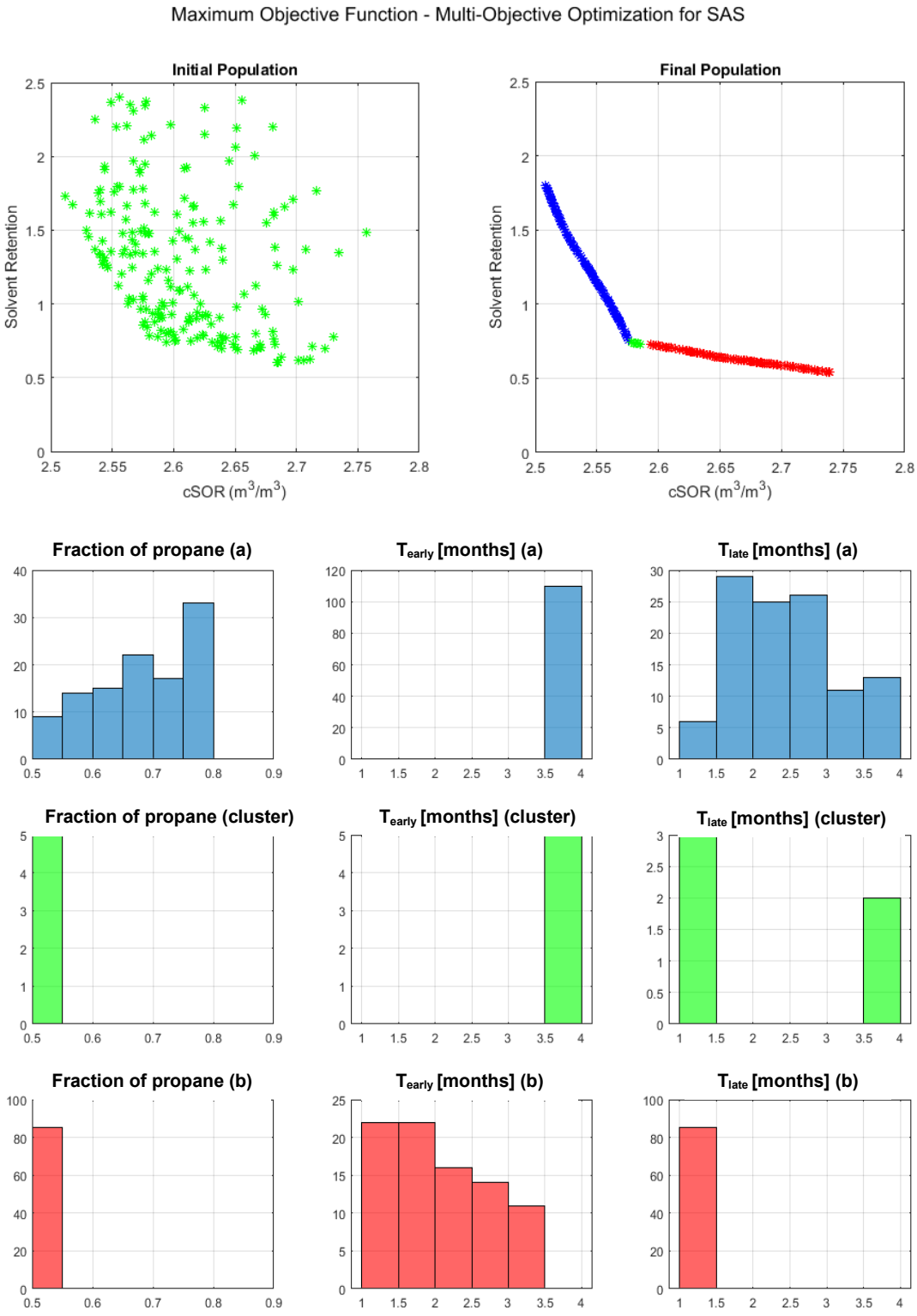

Figure 5.6—Pareto-front and histograms of decision parameters when the overall objective function is computed as the maximum among all 10 heterogeneous realizations: blue – region (a); red – region (b); green – new cluster.

After analyzing the results, we suggest to follow the operation conditions that the average-computed-objective-functions approach provides. This scenario is reliable due to the fact is more conservative, as we cannot predict exactly where the positions of the shale barriers in a real reservoir can be. We observed that the minimum approach represents or takes the values of the objective functions of the reservoir whit shale barriers far from the wells, and the maximum approach tends to utilize the values of the reservoirs with considerable presence near the wells region. Because this process has trade-off objective function values, the operational parameters cannot be a single value, that's why two ways to operate this process have been proposed and it depends on the availability of the resources in the field to take the decision of which set of operational parameters to use, because both options are optimal.

Compared to the homogeneous flow simulation, heterogeneous reservoirs are obviously more complex and requiring additional run time. The use of a proxy model has resulted in a significant reduction in computational costs. For instance, a single flow simulation run takes approximately 7 minutes, while it takes less than a second for the RSM to estimate each objective function. A limited number of initial models are required to calibrate these RSM proxy models; however, this front-end loading in computational costs can be easily justified, as it takes approximately two minutes using a personal computer [Intel(R) Core (TM) i7-3770 CPU (3.40 GHz) and 16 GB of installed memory (RAM)] to obtain a set of Pareto-optimal solutions from an initial population of 200. In contrast, if full flow simulations are required for each objective evaluation, the entire MOO workflow would take 972 days [100 iterations × 200 simulation runs per iteration × 7

minutes/simulation run × 10 reservoir realizations] to complete without any parallel computation.

Chapter 6 Conclusions and Recommendations

Conclusions from this study and recommendations for future study are provided in this Chapter.

6.1 Conclusions

A base homogeneous SAS simulation model is constructed using field data gathered from the Cold Lake region and compared with previous SAS simulation studies. A set of relevant decision variables is identified via a detailed sensitivity analysis using the base model. Two objective functions, including the solvent retention and cumulative steam-oil ratio (cSOR), are formulated. To incorporate the uncertainties due to reservoir heterogeneity, ten realizations of shale barrier distribution are created stochastically.

A novel hybrid optimization workflow is proposed to incorporate the uncertainties in objective functions introduced by the reservoir heterogeneities. The response surface methodology is employed to build a set of proxy models for the objective function evaluations. The NSGA-II multi-objective optimization (MOO) algorithm is employed to search for the optimal solutions. An overall function is defined for each of the two objective functions by aggregating individual values over all ten realizations based on the average, minimum, or maximum values. The NSGA-II identifies a reliable set of optimal decision parameters for the three approaches investigated in this work.

The optimization results reveal two distinct options for selecting the optimal decision parameters. For the first option, solvent is injected for longer periods during both

the early and late SAS stages, leading to higher recovery and lower steam injection (i.e., lower cSOR). The obvious trade-off is that there is likely to be higher solvent retention. For the second option, very little solvent is injected, so the solvent retention is low; however, more steam is injected, leading to higher *cSOR*. It is also noted that cases with higher objective function values are likely corresponding to those with more heterogeneities.

The proposed workflow for heterogeneous reservoirs can facilitate the identification of a set of Pareto-optimum solutions with considerable savings in computational costs. Future studies should include flexibility of duration of each cycle during the SAS process, because the workflow can be constrained too much with fixed and small ranges of solvent injection in the cycles.

6.2 Recommendations

For future studies, it would be important to consider applying different global optimization techniques and proxy methods.

A life cycle assessment of the SAS is recommended to verify the total negative impact to the environment, because in this study it was just considered the CO_2 emissions related to the of natural gas required to produce less steam compared to the traditional SAGD.

Also it should be important to consider flexibility of the duration of the cycles of steam and solvent injection to analyze the impacts on the results.

References

Alberta Energy Regulator (2015). Oil sands. (Accessed 10 February 2018) https://www.aer.ca/providing-information/by-topic/oil-sands

Al-Gosayir, M., Leung, J., & Babadagli, T. (2012). Design of solvent-assisted SAGD processes in heterogeneous reservoirs using hybrid optimization techniques. *Journal of Canadian Petroleum Technology*, 51(06), 437-448. https://doi.org/10.2118/149010-PA

Al-Gosayir, M., Leung, J., Babadagli, T., & Al Muatasim, M. (2013). Optimization of Steam-Over-Solvent Injection in Fractured Reservoirs (SOS-FR) method using hybrid techniques: Testing cyclic injection case. *Journal of Petroleum Science and Engineering*, 110, 74-84. https://doi.org/10.1016/j.petrol.2013.08.036

Amirian, E., Leung, J.Y., Zanon, S.D., and Dzurmann, P.J. (2014). Integrated cluster analysis and artificial neural network modeling for steam-assisted gravity drainage performance prediction in heterogeneous reservoirs. *Expert Systems with Applications* 42(2): 723-740. https://doi.org/10.1016/j.eswa.2014.08.034

Ali, S. M., & Blunschi, J. (1983). Cyclic Steam Stimulation With Formation Parting. In *Annual Technical Meeting*. Petroleum Society of Canada, Banff, Canada. https://doi.org/10.2118/83-34-45

Ardali, M., Barrufet, M., Mamora, D. D., & Qiu, F. (2012). A critical review of hybrid steam/solvent processes for the recovery of heavy oil and bitumen. In *SPE Annual*

Technical Conference and Exhibition. Society of Petroleum Engineers, San Antonio, USA. https://doi.org/10.2118/159257-MS

Coimbra, L., Ma, Z., & Leung, J. Y. (2019). Practical Application of Pareto-Based Multi-Objective Optimization and Proxy Modeling for Steam Alternating Solvent Process Design. In *SPE Western Regional Meeting*. Society of Petroleum Engineers. https://doi.org/10.2118/195247-MS

Deb, K. (2001). *Multi-objective optimization using evolutionary algorithms* (Vol. 16). John Wiley & Sons.

Deb, K., Pratap, A., Agarwal, S., & Meyarivan, T. A. M. T. (2002). A fast and elitist multiobjective genetic algorithm: NSGA-II. *IEEE transactions on evolutionary computation*, 6(2), 182-197.

Dobnikar, A., Steele, N. C., Pearson, D. W., & Albrecht, R. F. (Eds.). (2012). *Artificial Neural Nets and Genetic Algorithms: Proceedings of the International Conference in Portorož, Slovenia, 1999*. New York: Springer-Verlag Wien GmbH.

Donaldson, E. C., Chilingarian, G. V., & Yen, T. F. (Eds.). (1989). *Enhanced oil recovery, II: Processes and operations.* Elsevier.

Gupta, S. C., & Gittins, S. D. (2006). Christina Lake solvent aided process pilot. Journal of Canadian Petroleum Technology, 45(09).

Leung, J.Y. (2014). Scale-up of effective mass transfer in vapor extraction process accounting for field-scale reservoir heterogeneities, *Journal of Canadian Petroleum Technology,* 53(05), 275-289. https://doi.org/10.2118/153862-PA

Ma, Z., Leung, J.Y., Zanon, S., and Dzurman, P. (2015). Practical implementation of knowledge-based approaches for steam-assisted gravity drainage production analysis. *Expert Systems with Applications* 42(21): 7326-7343. https://doi.org/10.1016/j.eswa.2015.05.047

Ma, Z., Leung, J.Y., and Zanon, S.D. (2017). Practical data mining and artificial neural network modeling for SAGD production analysis. *Journal of Energy Resources Technology*, Transactions of the ASME 139(3): 03290. https://doi.org/10.1115/1.4035751

Ma, Z., Leung, J. Y., & Zanon, S. (2018). Integration of artificial intelligence and production data analysis for shale heterogeneity characterization in steam-assisted gravity-drainage reservoirs. *Journal of Petroleum Science and Engineering*, 163, 139-155. https://doi.org/10.1016/j.petrol.2017.12.046

Ma, Z. and Leung, J.Y. (2019). Integration of data-driven modeling techniques for lean zone and shale barrier characterization in SAGD reservoirs. *Journal of Petroleum Science and Engineering* 176: 716-734. https://doi.org/10.1016/j.petrol.2019.01.106

Ma, Z., & Leung, J. Y. (2019, March). Design of Warm Solvent Injection Processes for Heterogeneous Heavy Oil Reservoirs: A Hybrid Workflow of Multi-Objective Optimization and Proxy Models. In *SPE Reservoir Simulation Conference.* Society of Petroleum Engineers. https://doi.org/10.2118/193842-MS

Martin, W. L., Alexander, J. D., & Dew, J. N. (1958). Process variables of in situ combustion.

Min, B., Kang, J. M., Chung, S., Park, C., & Jang, I. (2014). Pareto-based multi-objective history matching with respect to individual production performance in a heterogeneous reservoir. *Journal of Petroleum Science and Engineering*, 122, 551-566. https://doi.org/10.1016/j.petrol.2014.08.023

Min, B., Kang, J. M., Lee, H., Jo, S., Park, C., & Jang, I. (2016). Development of a robust multi-objective history matching for reliable well-based production forecasts. *Energy Exploration & Exploitation*, 34(6), 795-809. https://doi.org/10.1177%2F0144598716665008

Min, B., Kannan, K., & Srinivasan, S. (2017). Quick Screening of Pareto-Optimal Operating Conditions for Expanding Solvent–Steam Assisted Gravity Drainage Using Hybrid Multi-Objective Optimization Approach. *Energies*, 10(7), 966. https://doi.org/10.3390/en10070966

Ngatchou, P., Zarei, A., & El-Sharkawi, A. (2005, November). Pareto multi objective optimization. In *Proceedings of the 13th International Conference on, Intelligent Systems Application to Power Systems* (pp. 84-91). IEEE. https://doi.org/10.1109/ISAP.2005.1599245

Schulze-Riegert, R. W., Krosche, M., Fahimuddin, A., & Ghedan, S. G. (2007). Multi-objective optimization with application to model validation and uncertainty quantification. In *SPE Middle East oil and gas show and conference*. Society of Petroleum Engineers. Manama, Bahrain. https://doi.org/10.2118/105313-MS

Shi, J., Vishal, V., and Leung, J.Y. (2014). Uncertainty assessment of vapex performance in heterogeneous reservoirs using a semi-analytical proxy model, *Journal of Petroleum Science and Engineering* 122: 290-303. https://doi.org/10.1016/j.petrol.2014.07.022

Souraki, Y., Torsater, O., Jahanbani Ghahfarokhi, A., & Ashrafi, M. (2013). Application of Solvent Alternating SAGD Process to Improve SAGD Performance in Athabasca Bitumen Reservoir. *In SPE Western Regional & AAPG Pacific Section Meeting 2013 Joint Technical Conference*. Society of Petroleum Engineers, Monterey, USA. https://doi.org/10.2118/165327-MS

Srinivas, N., & Deb, K. (1994). Muiltiobjective optimization using nondominated sorting in genetic algorithms. *Evolutionary computation*, 2(3), 221-248.

Wang, C., & Leung, J. (2015). Characterizing the effects of lean zones and shale distribution in steam-assisted-gravity-drainage recovery performance. *SPE Reservoir Evaluation & Engineering,* 18(03), 329-345. https://doi.org/10.2118/170101-PA

Wang, C., Ma, Z., Leung, J.Y., and Zanon, S. (2018). Correlating stochastically-distributed reservoir heterogeneities with steam-assisted gravity drainage production. *Oil & Gas Science and Technology – Revue d'IFP Energies nouvelles*, 73, 9. https://doi.org/10.2516/ogst/2017042

Zhao, L. (2007). Steam Alternating Solvent Process. *SPE Reservoir Evaluation & Engineering*, 10(02), 185-190. https://doi.org/10.2118/86957-PA

Zheng, J., Leung, J.Y., Sawatzky, R.P., and Alvarez, J.M. (2018). A proxy model for predicting SAGD production from reservoirs containing shale barriers. *Journal of*

Energy Resources Technology, Transactions of the ASME 140(12): 122903. https://doi.org/10.1115/1.4041089

Zheng, J., Leung, J. Y., Sawatzky, R. P., & Alvarez, J. M. (2019). An AI-based workflow for estimating shale barrier configurations from SAGD production histories. *Neural Computing and Applications*, 31(9), 5273-5297. https://doi.org/10.1007/s00521-018-3365-9

Appendices

Appendix 1: Sensitivity Analysis

In this section, several figures of cumulative oil produced obtained during the sensitivity analysis for different ranges of operational parameters tested are presented. It has been observed the differences during the period of 3 years, at the end of the first year of SAS stage.

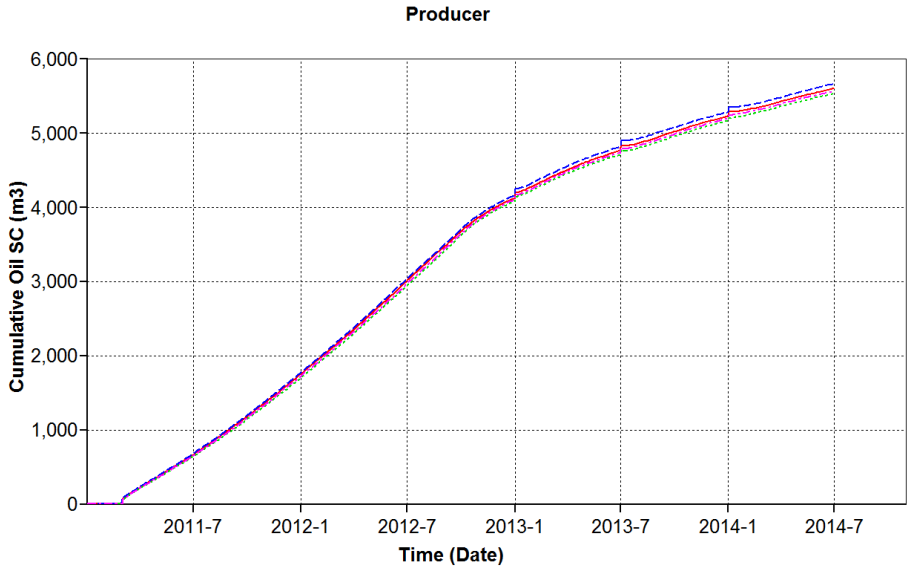

a) Steam trap

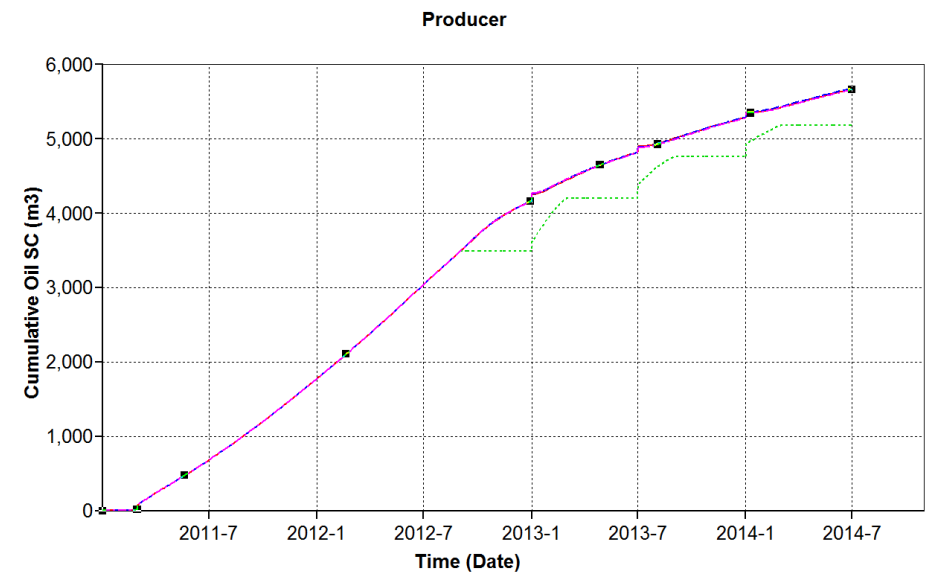

b) Bottom-hole gas (m^3)

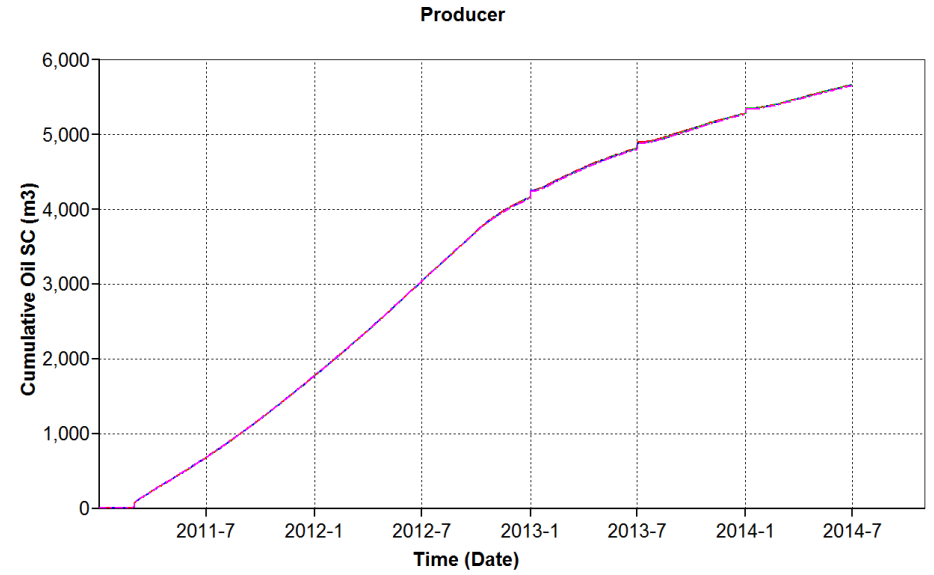

c) Temperature of injected fluids (°C)

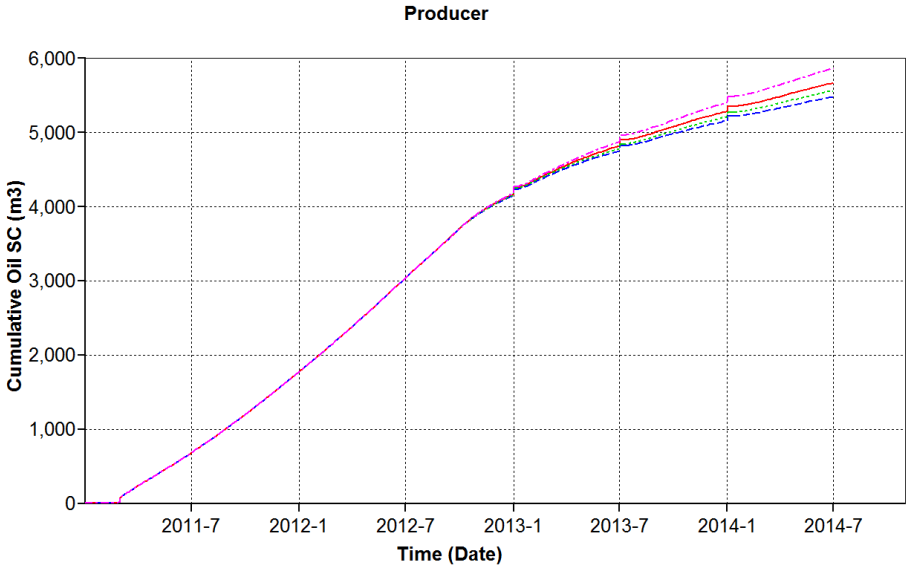

d) Fraction of propane in the solvent

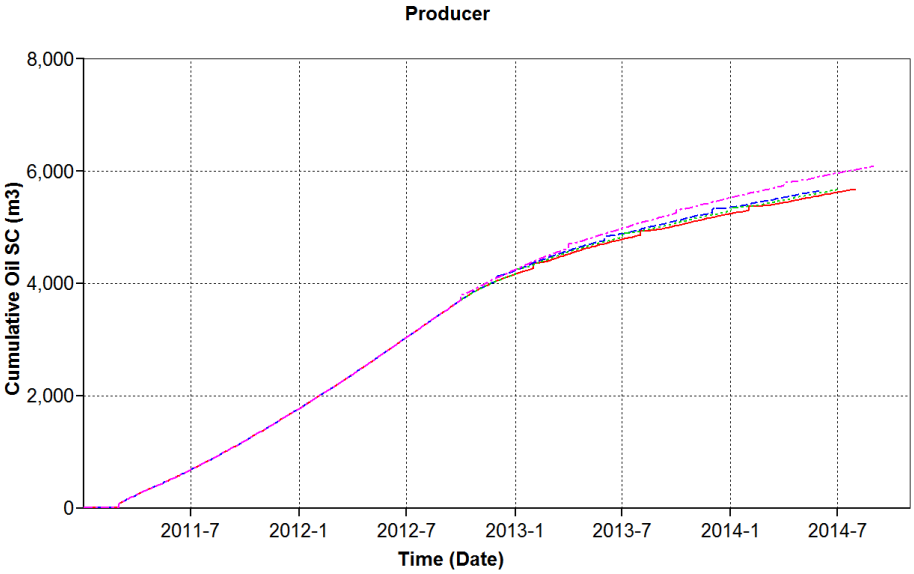

e) Duration of solvent injection in each cycle (months)

Appendix 2: Dataset used in proxy model construction for the two-objectives homogeneous case

Case #	$F_{propane}$	T_{early} (months)	T_{late} (months)	*cSOR* (m^3/m^3)	$Propane_{retention}$ *normalized*
1	0.50	1	1	2.404	0.365
2	0.50	1	2	2.368	0.454
3	0.50	1	3	2.333	0.547
4	0.50	1	4	2.290	0.625
5	0.50	2	1	2.341	0.456
6	0.50	2	2	2.312	0.526
7	0.50	2	3	2.294	0.622
8	0.50	2	4	2.252	0.688
9	0.50	3	1	2.282	0.518
10	0.50	3	2	2.274	0.586
11	0.50	3	3	2.255	0.681
12	0.50	3	4	2.211	0.740
13	0.50	4	1	2.252	0.594
14	0.50	4	2	2.247	0.650
15	0.50	4	3	2.230	0.725
16	0.50	4	4	2.191	0.785
17	0.55	1	1	2.407	0.416
18	0.55	1	2	2.375	0.519
19	0.55	1	3	2.338	0.638
20	0.55	1	4	2.285	0.712
21	0.55	2	1	2.348	0.540
22	0.55	2	2	2.323	0.644
23	0.55	2	3	2.297	0.737
24	0.55	2	4	2.257	0.819

25	0.55	3	1	2.303	0.606
26	0.55	3	2	2.289	0.697
27	0.55	3	3	2.267	0.788
28	0.55	3	4	2.228	0.873
29	0.55	4	1	2.255	0.681
30	0.55	4	2	2.247	0.759
31	0.55	4	3	2.237	0.838
32	0.55	4	4	2.197	0.922
33	0.60	1	1	2.420	0.462
34	0.60	1	2	2.377	0.581
35	0.60	1	3	2.342	0.740
36	0.60	1	4	2.294	0.833
37	0.60	2	1	2.342	0.574
38	0.60	2	2	2.326	0.700
39	0.60	2	3	2.299	0.826
40	0.60	2	4	2.246	0.919
41	0.60	3	1	2.322	0.706
42	0.60	3	2	2.308	0.804
43	0.60	3	3	2.285	0.933
44	0.60	3	4	2.244	1.008
45	0.60	4	1	2.271	0.790
46	0.60	4	2	2.257	0.867
47	0.60	4	3	2.253	0.983
48	0.60	4	4	2.204	1.056
49	0.65	1	1	2.421	0.514
50	0.65	1	2	2.382	0.672
51	0.65	1	3	2.336	0.797
52	0.65	1	4	2.302	0.963
53	0.65	2	1	2.351	0.663

54	0.65	2	2	2.326	0.787
55	0.65	2	3	2.296	0.922
56	0.65	2	4	2.246	1.048
57	0.65	3	1	2.306	0.818
58	0.65	3	2	2.299	0.938
59	0.65	3	3	2.271	1.046
60	0.65	3	4	2.237	1.182
61	0.65	4	1	2.258	0.910
62	0.65	4	2	2.247	0.989
63	0.65	4	3	2.228	1.149
64	0.65	4	4	2.202	1.239
65	0.70	1	1	2.426	0.561
66	0.70	1	2	2.386	0.743
67	0.70	1	3	2.354	0.916
68	0.70	1	4	2.303	1.105
69	0.70	2	1	2.359	0.753
70	0.70	2	2	2.331	0.893
71	0.70	2	3	2.308	1.067
72	0.70	2	4	2.260	1.244
73	0.70	3	1	2.299	0.895
74	0.70	3	2	2.281	1.036
75	0.70	3	3	2.252	1.180
76	0.70	3	4	2.223	1.328
77	0.70	4	1	2.256	1.011
78	0.70	4	2	2.239	1.112
79	0.70	4	3	2.232	1.264
80	0.70	4	4	2.189	1.391
81	0.75	1	1	2.429	0.618
82	0.75	1	2	2.393	0.814

83	0.75	1	3	2.354	1.033
84	0.75	1	4	2.298	1.243
85	0.75	2	1	2.365	0.867
86	0.75	2	2	2.328	0.986
87	0.75	2	3	2.293	1.208
88	0.75	2	4	2.258	1.425
89	0.75	3	1	2.296	1.013
90	0.75	3	2	2.278	1.132
91	0.75	3	3	2.264	1.328
92	0.75	3	4	2.220	1.506
93	0.75	4	1	2.264	1.194
94	0.75	4	2	2.258	1.286
95	0.75	4	3	2.233	1.451
96	0.75	4	4	2.203	1.587
97	0.80	1	1	2.434	0.691
98	0.80	1	2	2.400	0.941
99	0.80	1	3	2.345	1.135
100	0.80	1	4	2.289	1.419
101	0.80	2	1	2.365	0.953
102	0.80	2	2	2.333	1.115
103	0.80	2	3	2.306	1.336
104	0.80	2	4	2.250	1.551
105	0.80	3	1	2.299	1.156
106	0.80	3	2	2.286	1.307
107	0.80	3	3	2.262	1.503
108	0.80	3	4	2.226	1.719
109	0.80	4	1	2.247	1.383
110	0.80	4	2	2.240	1.495
111	0.80	4	3	2.224	1.653

112	0.80	4	4	2.196	1.829
113	0.85	1	1	2.433	0.739
114	0.85	1	2	2.397	1.035
115	0.85	1	3	2.352	1.273
116	0.85	1	4	2.287	1.570
117	0.85	2	1	2.360	1.021
118	0.85	2	2	2.335	1.228
119	0.85	2	3	2.294	1.466
120	0.85	2	4	2.252	1.782
121	0.85	3	1	2.292	1.315
122	0.85	3	2	2.280	1.471
123	0.85	3	3	2.258	1.701
124	0.85	3	4	2.205	2.002
125	0.85	4	1	2.247	1.619
126	0.85	4	2	2.244	1.740
127	0.85	4	3	2.230	1.937
128	0.85	4	4	2.175	2.191
129	0.90	1	1	2.440	0.833
130	0.90	1	2	2.405	1.131
131	0.90	1	3	2.357	1.497
132	0.90	1	4	2.289	1.837
133	0.90	2	1	2.360	1.152
134	0.90	2	2	2.331	1.380
135	0.90	2	3	2.293	1.669
136	0.90	2	4	2.239	2.036
137	0.90	3	1	2.309	1.517
138	0.90	3	2	2.282	1.697
139	0.90	3	3	2.254	1.960
140	0.90	3	4	2.211	2.271

141	0.90	4	1	2.229	1.877
142	0.90	4	2	2.221	2.008
143	0.90	4	3	2.201	2.209
144	0.90	4	4	2.167	2.488

Appendix 3: Results of Proxy modeling for the two-objectives homogeneous case

RSM coefficients	*cSOR* *(m^3/m^3)*	*$Propane_{retention}$* *(normalized)*
β_0	2.2938	1.5525
β_1	0.5134	-4.2337
β_2	-0.0571	-0.1378
β_3	-0.0088	-0.1686
β_{12}	-0.0379	0.5213
β_{12}	-0.0187	0.4782
β_{23}	0.0078	-0.0197
β_{11}	-0.2652	3.1970
β_{22}	0.0041	-0.0065
β_{33}	-0.0057	0.0086